Early Neoproterozoic (Tonian) subduction-related magmatism and tectonothermal activity in Shetland and northern mainland Scotland: implications for the tectonic evolution of NE Laurentia and Rodinia reconstructions

P. D. Kinny[1], R. A. Strachan[2]*, M. B. Fowler[2], E. Bruand[3], I. L. Millar[4], M. Hand[5], C. Clark[1] and K. A. Cutts[6]

[1] The Institute for Geoscience Research, Curtin University, GPO U1987, Perth, WA 6845, Australia
[2] School of the Environment and Life Sciences, Geography and Geosciences, University of Portsmouth, Burnaby Road, Portsmouth, PO1 3QL, UK
[3] Geo-Ocean, UMR6538, CNRS, Université Brest, IFREMER, Plouzané, France
[4] NERC Isotope Geoscience Laboratories, Keyworth, Nottingham, NG12 5GG, UK
[5] School of Earth and Environmental Sciences, University of Adelaide, SA 5005, Australia
[6] Geological Survey of Finland, P.O. Box 96, F1-02151 Espoo, Finland

RAS, 0000-0002-9568-0832
* Correspondence: rob.strachan@port.ac.uk

Abstract: The tectonic setting of Tonian orogenic events recorded in the present-day circum-North Atlantic region is uncertain. U–Pb zircon geochronology shows that the Yell Sound and Westings groups (Shetland) and metasedimentary rocks of the Naver Nappe (northern mainland Scotland) were deposited between *c.* 1050 and 960 Ma and intruded by mafic, intermediate and felsic igneous rocks at *c.* 965–950 Ma. Chemical discrimination diagrams and Hf and Nd isotope data together suggest that the protoliths of the mafic meta-igneous rocks were emplaced as relatively juvenile crustal contributions in an active plate margin. Zircon growth at *c.* 920 Ma within the Yell Sound Group correlates with high-grade metamorphism documented previously in Shetland. Further zircon growth and Pb loss at *c.* 470–460 Ma indicates overprinting during the Ordovician Grampian orogenic event. Similar age successions of Ellesmere Island, Svalbard and East Greenland also contain evidence for Tonian magmatism (some calc-alkaline), deformation and metamorphism. The new data favour Rodinia reconstructions that incorporate subduction-related magmatism and associated tectonism along the margin of NE Laurentia during the Tonian. The Yell Sound Group and correlative peri-Laurentian successions were intruded by subduction-related magmas and deformed and metamorphosed during development of the Valhalla exterior accretionary orogen, part of a more extensive peri-Rodinian subduction system.

Supplementary material: Supplementary data tables and a figure are available at https://doi.org/10.6084/m9.figshare.c.7405471

Received 11 May 2024; **revised** 7 August 2024; **accepted** 15 August 2024

A widely accepted view is that the assembly of the supercontinent Rodinia culminated in the collision of Laurentia, Baltica and Amazonia, and development of the Grenvillian and Sveconorwegian orogens at *c.* 1.2–1.0 Ga (Fig. 1; e.g. Dalziel 1991; Hoffman 1991; Weil *et al.* 1998; Torsvik 2003; Bingen *et al.* 2008, 2021; Gower *et al.* 2008; Li *et al.* 2008; Cawood and Pisarevsky 2017). In this context, the tectonic significance of Tonian orogenic events recorded in Ellesmere Island, East Greenland, Norway, Svalbard, Shetland and NW Scotland (Gee *et al.* 1995; Strachan *et al.* 1995; Watt and Thrane 2001; Leslie and Nutman 2003; Johansson *et al.* 2005; Kirkland *et al.* 2006, 2007, 2008*a*; Cutts *et al.* 2009*a, b*, 2010; Pettersson *et al.* 2009; Malone *et al.* 2014, 2017; Jahn *et al.* 2017; Bird *et al.* 2018) is less well understood. Tonian palaeocontinental reconstructions differ in the relative locations of Baltica and Laurentia. The most widely cited places western Baltica opposite Rockall Bank (Fig. 1; Cawood and Pisarevsky 2006, 2017; Li *et al.* 2008; Johansson 2009, 2014, 2016; Elming *et al.* 2014). In this interpretation, Tonian orogenic events in NE Laurentia resulted from the development after *c.* 1 Ga of the Valhalla accretionary orogen (Cawood *et al.* 2010, 2015; see also Bingen *et al.* 2011, 2020; Kirkland *et al.* 2011; Gasser and Andresen 2013; Malone *et al.* 2014, 2017). This is thought to have been part of an extensive peri-Rodinian subduction system (Cawood *et al.* 2016; Ge *et al.* 2016;

Štípská *et al.* 2023), which may have included Siberia where convergent margin activity commenced at *c.* 970–940 Ma (Fig. 1; Pease *et al.* 2001; Vernikovsky *et al.* 2011). However, other reconstructions place East Greenland directly opposite western Baltica following a putative collision at *c.* 1 Ga (Lorenz *et al.* 2012; Gee *et al.* 2015), or possibly Baltica never formed part of Rodinia (Kulakov *et al.* 2022; Slagstad *et al.* 2023; Slagstad and Kulakov 2024).

The distinction between collisional and accretionary orogens in the Precambrian is often problematic, particularly within the North Atlantic borderlands, because most Neoproterozoic rock units were strongly deformed and metamorphosed during the Ordovician–Silurian Caledonian orogeny. Nonetheless, three major cycles of Neoproterozoic sedimentation and tectonic activity have been identified in NE Laurentia (Cawood *et al.* 2007, 2010, 2015; Kirkland *et al.* 2008*b*; Olierook *et al.* 2020). The oldest is represented by *c.* 1000 Ma siliciclastic sequences preserved in Svalbard, East Greenland and Scotland, and also in Laurentian-derived allochthons in northern Norway. Sedimentation overlapped the final stages of the assembly of Rodinia and these sequences all contain detritus sourced from the Grenvillian and Sveconorwegian orogens. Deformation and amphibolite-facies metamorphism occurred between 980 and 920 Ma (the 'Renlandian' event of

Fig. 1. Palaeogeographical reconstruction for *c.* 990 Ma. Red line shows the extent of the collisional Grenvillian–Sveconorwegian orogen; dashed green line with triangles shows peri-Rodinian subduction zones; blue line indicates a passive margin adjacent to (present-day) northern Baltica. Au, Australia; Si, Siberia; La, Laurentia; P, Pearya (Ellesmere Island); Sv, Svalbard; EG, East Greenland; S, Scotland (including Shetland); Ba, Baltica; RP, Rio Plata craton; Am, Amazonia; WA, West African craton. Source: modified from Cawood *et al.* (2016).

Cawood *et al.* 2010). Early Neoproterozoic calc-alkaline igneous suites in Ellesmere Island (Malone *et al.* 2017), eastern Svalbard (Johansson *et al.* 1999, 2004, 2005) and within Laurentia-derived allochthons of northern Norway (Kirkland *et al.* 2006, 2007) imply proximity of some of these basins to an active plate margin. An intermediate cycle incorporates successions in Scotland and northern Norway that accumulated after *c.* 900 Ma and record multiple mid-Neoproterozoic tectonothermal events, commonly grouped in Scotland as 'Knoydartian' (Rogers *et al.* 1998; Vance *et al.* 1998; Cutts *et al.* 2009*a*, 2010; Cawood *et al.* 2010, 2015, see also Kirkland *et al.* 2007, 2008*a*, 2011). The youngest cycle comprises late Neoproterozoic to early Paleozoic units preserved in East Greenland, Svalbard and Scotland that were deposited prior to and during the main phase of Rodinia break-up.

Notwithstanding the broad tectonostratigraphic framework outlined above, the age and tectonic evolution of many Neoproterozoic metasedimentary successions and associated igneous suites in the North Atlantic borderlands are still uncertain. Shetland (Fig. 2) formed part of the Laurentia palaeocontinent and occupies a key link between the East Greenland, Scottish and Norwegian parts of the Caledonides in pre-Mesozoic reconstructions. Aspects of the pre-Devonian geology of Shetland have been the focus of recent geochronological–metamorphic studies (Cutts *et al.* 2009*b*, 2011; Strachan *et al.* 2013; Walker *et al.* 2016, 2021; Jahn *et al.* 2017; Kinny *et al.* 2019) but constraints on the ages and tectonic significance of many rock units are still lacking. We have therefore carried out U–Pb zircon dating on metasedimentary rocks and a range of mafic, intermediate and felsic meta-igneous rocks on Shetland. For comparative purposes we have also carried out U–Pb zircon dating on an early meta-igneous complex in the Caledonides of mainland northern Scotland. Trace element, Nd, Sr and Hf isotopic data obtained from meta-igneous rocks in both areas shed light on the character and tectonic setting of magmatism. The data support a revised tectonostratigraphic framework for the early Neoproterozoic rocks of Shetland and northern mainland Scotland

and provide further constraints on regional correlations within the circum-North Atlantic region and palaeocontinental reconstructions for this segment of Rodinia.

Geological setting

Caledonian framework and regional correlations between Shetland and mainland northern Scotland

The Ordovician–Silurian Caledonide orogen of Scotland is dominated by mainly Neoproterozoic metasedimentary successions that were deformed and metamorphosed at *c.* 470–430 Ma (Strachan *et al.* 2002, 2010*b*, 2024*b*; Chew and Strachan 2014; Law *et al.* 2024; Leslie *et al.* 2024; Prave *et al.* 2024). The Caledonides are limited by the Moine Thrust in mainland northern Scotland (Fig. 2a), and the equivalent structure in Shetland is likely to be the Uyea Shear Zone (Fig. 2b; Walker *et al.* 2016, 2021; Kinny *et al.* 2019). The Neoarchean Lewisian Gneiss Complex of the Caledonian foreland in mainland northern Scotland is structurally analogous to the similar-aged Uyea Gneiss Complex in NW Shetland (Fig. 2b; Flinn 1985; Kinny *et al.* 2019) and correlative basement on the adjacent continental shelf (Holdsworth *et al.* 2019; Strachan *et al.* 2024*a*). The early Neoproterozoic Moine Supergroup of Holdsworth *et al.* (1994) dominates the bedrock geology of mainland northern Scotland (Northern Highland Terrane; Fig. 2a), although it has now been redefined as comprising units belonging to two separate supergroups (Wester Ross and Loch Ness supergroups) separated by an orogenic unconformity (Krabbendam *et al.* 2021). Potential correlatives of the Moine rocks *sensu lato* in Shetland are the Sand Voe, Yell Sound and Westing groups (Fig. 2b; Flinn 1985, 1988, 1994). Between the Great Glen and Highland Boundary faults in mainland Scotland (Grampian Terrane; Fig. 2a), the bedrock geology is dominated by the middle Neoproterozoic to Cambrian Dalradian Supergroup, which was deposited during the break-up of Rodinia after *c.* 750 Ma and development of the Iapetus Ocean (Prave *et al.* 2024). The likely correlative unit in Shetland is the East Mainland Succession (Fig. 2b; Flinn 2007; Strachan *et al.* 2013).

Shetland Islands

Contrasting but approximately contemporaneous early Neoproterozoic metasedimentary successions crop out in the NE of the Shetland Islands: the Yell Sound and Westing groups (Fig. 2b). The Yell Sound Group is dominated by gneissic, often migmatitic, metapsammites with subordinate meta-semipelites and quartzites and has a structural thickness of *c.* 10 km (Flinn 1994). The Westing Group is dominated by gneissic and migmatitic metapelites with subordinate meta-semipelites and marble (Flinn 2014) and has a structural thickness of *c.* 100–200 m. No sedimentary structures are visible in either unit, and the order of succession is unknown. Granitic orthogneisses and amphibolite intrusions were emplaced either prior to or during the earliest tectonic events (Flinn 1994, 2014). Lower age limits on deposition are provided by the ages of youngest detrital zircons, which are *c.* 1030 Ma (Westing Group, Cutts *et al.* 2009*b*) and *c.* 1019 Ma (Yell Sound Group, Jahn *et al.* 2017). Upper age limits are provided by evidence for high-grade metamorphism at *c.* 938–925 Ma (Westing Group, Cutts *et al.* 2009*b*) and *c.* 944–931 Ma (Yell Sound Group, Jahn *et al.* 2017). Petrological studies and mineral age dating demonstrate widespread Ordovician (*c.* 470–450 Ma) reworking at *P–T* conditions up to 10 kbar and 775°C (Cutts *et al.* 2011; Walker *et al.* 2016, 2021).

Extensive occurrences of dominantly mafic orthogneisses with interbanded amphibolite on Yell and the Walls Peninsula, and between Fethaland and Ronas Voe in NW Shetland (Fig. 2b, 'orthogneisses of uncertain affinities') have been considered mainly
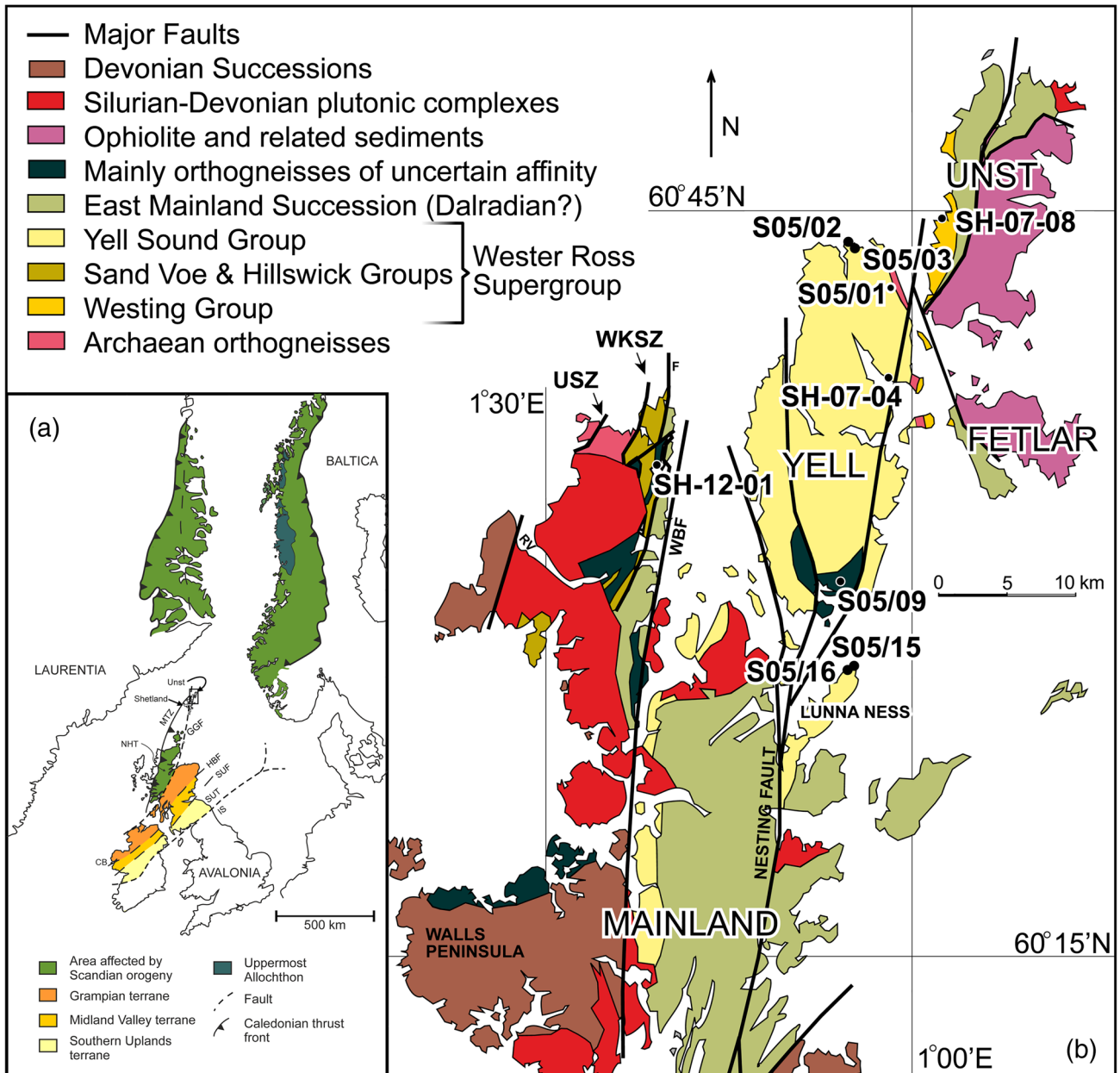
Fig. 2. (a) Location of the Shetland Islands relative to mainland Scotland, Greenland and Scandinavia prior to opening of the North Atlantic Ocean. MTZ, Moine Thrust Zone; NHT, Northern Highland terrane; GGF, Great Glen Fault; HBF, Highland Boundary Fault; SUF, Southern Uplands Fault; SUT, Southern Uplands terrane; IS, Iapetus Suture; CB, Clew Bay. **(b)** Geology of northern Shetland showing the location of samples for U–Pb zircon geochronology. USZ, Uyea Shear Zone; RV, Ronas Voe; F, Fethaland; WBF, Walls Boundary Fault; WKSZ, Wester Keolka Shear Zone; other abbreviations as for **(a)**.

on lithological grounds to be inliers of either Archean ('Lewisianoid') or Proterozoic basement on which the sedimentary protoliths of the Yell Sound, Westing and Sand Voe groups were deposited (Flinn *et al.* 1979; Flinn 1985, 1988, 1994). However, no basal conglomerates are present within adjacent metasedimentary successions, and there are no visible discordances across the proposed 'basement–cover' contacts. To date, the only orthogneisses east of the Wester Keolka Shear Zone that have proven basement affinities are those in NE Yell (Fig. 2b), which have yielded Neoarchean protolith ages (Jahn *et al.* 2017).

Mainland northern Scotland

The metasedimentary rocks of the Naver Nappe in mainland northern Scotland (Fig. 3) have traditionally been assigned to the Moine Supergroup (Holdsworth *et al.* 1994) and are now regarded as part of

the newly designated Wester Ross Supergroup (Krabbendam *et al.* 2021). They comprise gneissic and migmatitic metapsammites and metapelites (Moorhouse and Moorhouse 1988; Strachan and Holdsworth 1988; Burns 1994; Holdsworth *et al.* 2001). The U–Pb age of the youngest detrital zircon is 1005 ± 18 Ma (Kinny *et al.* 1999). No sedimentary structures are preserved and the order of succession is unknown. Tectonic slices and infolds of hornblende gneisses are interpreted as inliers of Lewisianoid basement, and one of these has yielded indications of a Neoarchean protolith age (Friend *et al.* 2008). The Druim Chuibhe Orthogneiss Complex (Fig. 3) is a series of interbanded, intermediate to felsic orthogneisses and amphibolites, which is thought to have been emplaced at an early stage in the polyphase tectonic history of the host paragneisses (Burns 1994; Strachan *et al.* 2010a). U–Pb zircon data indicate that migmatization of the host paragneisses occurred during the Caledonian orogeny at *c.* 470–460 Ma (Kinny *et al.* 1999). Peak
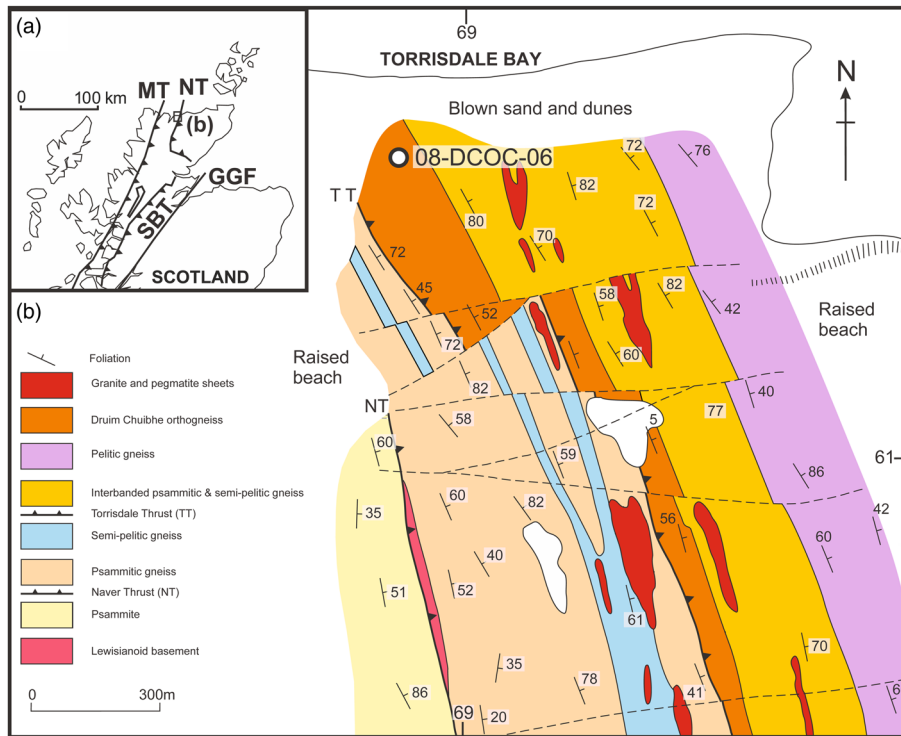
Fig. 3. (**a**) Inset shows location of the main map on the north coast of Scotland. MT, Moine Thrust; NT, Naver Thrust; SBT, Sgurr Beag Thrust; GGF, Great Glen Fault. (**b**) Detailed map and structural setting of the Druim Chuibhe Orthogneiss Complex and host metasedimentary rocks showing location of sample for U–Pb zircon geochronology. Source: modified from Strachan *et al.* (2010*a*).

Caledonian pressure–temperature conditions are estimated at 11–12 kbar and 650–700°C (Friend *et al.* 2000).

Sample characteristics and field relations

Yell Sound Group metapelites

S05/02 Brim Ness semi-pelitic gneiss, sampled at [HU 51698 05331]

This is a coarse-grained metapelite composed of quartz, plagioclase, K-feldspar, biotite, muscovite and garnet with accessory opaque minerals and zircon. Garnet porphyroblasts are up to 10 mm in diameter, and are often rich in quartz inclusions. A regular stromatic migmatitic fabric is imparted by the presence of centimetre-scale quartzo-feldspathic segregations forming discrete bands and lenticles.

SH-07-04 Kirkrabister pelite, sampled at [HU 54388 95501]

This is a coarse-grained metapelite composed of quartz, plagioclase, K-feldspar, biotite, muscovite and garnet with accessory opaque minerals and zircon. Distinctive centimetre-scale quartzo-feldspathic augen commonly contain 3–5 mm diameter garnet porphyroblasts and are wrapped by an anastomosing late muscovite shear fabric. Garnets are commonly embayed and inclusion-rich, and are locally replaced by chlorite.

S05/15 Lunna Ness migmatitic gneiss, sampled at [HU 51848 74108]

The locality sampled is dominated by highly migmatized metapsammites and metapelites, which contain numerous concordant metre- to centimetre-scale boudins of garnet-amphibolite. The sample is a medium- to coarse-grained metapelite that contains garnet, biotite, plagioclase, K-feldspar and quartz with accessory ilmenite and zircon. Garnet grains are up to 3 mm in size, commonly skeletal, embayed and replaced by aggregates of biotite and quartz.

Felsic orthogneiss intrusions within the Yell Sound Group

S05/16 Valayre granitic gneiss, sampled at [HU 51630 74087]

The term 'Valayre Gneiss' was employed by Flinn (1988, 1994) to refer to occurrences of augen gneiss developed close to the boundary of the Yell Sound Group with the East Mainland Succession (Fig. 2b). The characteristic feature of the 'Valayre Gneiss' is the presence of centimetre-scale microcline megacrysts (Fig. 4a) that vary from rounded to augen in shape and are only rarely rectangular. Flinn (1994) argued that the gneiss is not a single lithological unit, but the result of the growth of microcline porphyroblasts in a range of protolith lithologies. On the peninsula of Lunna Ness (Fig. 2b) the 'Valayre Gneiss' is a foliated, migmatitic granitoid that has a structural thickness of *c.* 150–200 m and is traceable laterally for 7 km (British Geological Survey 1981). Contacts between the 'Valayre Gneiss' and host Yell Sound Group rocks are concordant and sharp. The 'Valayre Gneiss' contains metre- to centimetre-scale boudins and lenses of garnet-amphibolite, one of which has a particularly distinctive rectangular shape and is interpreted here as a xenolith (Fig. 4b). We therefore consider that at least in Lunna Ness the 'Valayre Gneiss' is a deformed and metamorphosed granite, and accordingly refer to it henceforth as the 'Valayre granitic gneiss'. The sample comprises a medium-grained assemblage of quartz, plagioclase, biotite, muscovite and garnet with large (up to 3 cm) microcline augen, and accessory ilmenite and zircon.

S05/01 Gutcher granitic gneiss, sampled at [HU 54967 99595]

The Gutcher granitic gneiss intrudes the Yell Sound Group in NE Yell (Fig. 2b). It has a structural thickness of a few tens of metres and its contacts are poorly exposed. It is likely to pass transitionally northwards into a *c.* 150 m thick sheet of augen gneiss mapped as 'Valayre Gneiss' and traceable intermittently to the north coast of Yell (British Geological Survey 1994). The sample is composed of quartz, biotite, muscovite, plagioclase and K-feldspar with

Fig. 4. (**a**) Valayre granitic gneiss showing rounded microcline megacrysts, quarry by Loch of Grutwick [HU 504 707]; (**b**) rectangular xenolith of amphibolites within Valayre granitic gneiss, Lunna Ness [HU 5186 7412]; (**c**) typical appearance of the Gutcher granitic gneiss, showing lenticular augen of K-feldspar, Gutcher Quarry, NE Yell [HU 54967 99595]; (**d**) Breckon granitic gneiss displaying stromatic migmatitic banding, west of Breckon Sand, north Yell [HP 52415 04969]; (**e**) coarsely banded mafic orthogneiss, Houlland Quarry [HU 5061 8008]; (**f**) deformed magma mingling textures within the Kirkaby orthogneiss, west Unst [HU 5677 0660]; (**g**) intermediate orthogneiss of the Drium Chuibhe Orthogneiss Complex, Torrisdale Bay [NC 6887 6170]; (**h**) irregular inclusions of amphibolite within Valayre granitic gneiss, Lunna Ness [HU 5184 7410].

accessory garnet, titanite and zircon. Grain size is fine to medium. Centimetre-scale quartzo-feldspathic segregations and layers impart a well-developed gneissic fabric (Fig. 4c).

S05/03 Breckon granitic gneiss, sampled at [HU 52415 04969]

The Breckon granitic gneiss intrudes the Yell Sound Group in north Yell and has a structural thickness of *c.* 500–600 m. It has sharp contacts with host metasediments. The Yell Sound Group contains relic andalusite at two localities adjacent to the intrusion, perhaps indicative of an early thermal aureole (Flinn 1994). Grain size is typically medium and relatively uniform. Semi-continuous layers of quartzo-feldspathic segregations up to 1–1.5 cm thick impart a planar stromatic banding in parts of the outcrop (Fig. 4d). The sample comprises variable proportions of quartz, biotite, plagioclase and K-feldspar with accessory garnet, titanite and zircon.

Interbanded mafic and felsic orthogneiss within the Yell Sound and Sand Voe groups (= 'orthogneisses of uncertain affinity')

S05/09 Houlland mafic orthogneiss, sampled at Houlland Quarry [HU 5061 8008]

The Houlland orthogneisses have a structural thickness of at least 1 km, although contacts with the Yell Sound Group are poorly exposed. The dominant lithology is coarse-grained, mafic, hornblende gneiss with layers and pods up to a metre thick of amphibolite. The mafic gneiss is not prominently banded, the gneissic fabric mainly being defined by subparallel centimetre-scale wisps and lenticles of quartzo-feldspathic material. Distinct layering is imparted locally by pyroxene- and epidote-rich layers (Flinn 1994). In places the mafic gneiss passes transitionally into 3–4 m thick layers of intermediate gneiss by increase in proportion of felsic minerals. Rare areas of low strain preserve relics of original intrusive

relationships between different mafic phases, and the local interdigitation of diffuse patches and lenses of mafic and felsic variants suggests that contrasting protolith magmas were contemporaneous. Coarse garnet–biotite quartzo-feldspathic felsic orthogneiss forms a subordinate part of the inlier. A prominent banding is typically imparted by 1–2 cm scale quartz–feldspar layers, in places enhanced by augen texture formed by elongate, recrystallized feldspars. The sample is a mafic orthogneiss composed of granoblastic hornblende, plagioclase and quartz with accessory titanite and zircon. Grain size is medium and a gneissosity is imparted by quartzo-feldspathic layers and lenticles (Fig. 4e). A range of mafic orthogneisses was sampled for chemistry.

SH12-01 Burra Voe felsic orthogneiss, sampled at [HU 3726 8929]

The Burra Voe orthogneiss is traceable semi-continuously for a strike length of *c.* 15 km between Fethaland in the north southwards to Ronas Voe (Fig. 2b; British Geological Survey 2004). The northernmost segment north of Burra Voe is relatively mafic and dominated by interbanded hornblende gneiss and amphibolite. Banding is typically developed on a scale of 20–30 cm and defined by variations in the proportions of hornblende, biotite, plagioclase and quartz, with garnet locally common. All lithologies are cut by diffuse sheets of deformed quartz–feldspar pegmatite. South of Burra Voe, the orthogneiss also includes banded, medium-grained biotite–quartz–feldspar felsic gneiss with occasional metre-scale pods of amphibolite. Compositional banding on a scale of 1–5 cm is enhanced by parallel layers of deformed quartzo-feldspathic pegmatite and abundant feldspar augen. Contacts between the orthogneiss and the Sand Voe Group are invariably concordant and locally highly strained. The sample is a felsic gneiss composed of a medium-grained assemblage of quartz, plagioclase, garnet and muscovite with accessory titanite and zircon. Aligned laths of muscovite define a well-developed planar fabric. A range of mafic orthogneisses was also sampled for chemistry.

Interbanded mafic and felsic orthogneiss within the Westing Group

SH-07-08 Kirkaby felsic orthogneiss, sampled at [HU 5682 0666]

The intrusive complex comprises interbanded mafic and felsic orthogneiss with a structural thickness of *c.* 80–100 m. The dominant lithology is medium- to coarse-grained mafic orthogneiss with subordinate concordant sheets of felsic orthogneiss up to 0.5–1 m in thickness. The mafic orthogneiss is often intensely permeated by centimetre-scale quartzo-feldspathic veins that enclose pods and lenses of mafic material. Even though all components are deformed, outcrop-scale relationships (Fig. 4f) and preserved crenulate margins at the interface between mafic and felsic components are suggestive of magma mingling. The sample is a felsic orthogneiss that comprised plagioclase, K-feldspar, quartz and biotite with accessory garnet, titanite, opaque minerals and zircon. A range of mafic orthogneisses was also sampled for chemistry.

Druim Chuibhe Orthogneiss Complex (Naver nappe, mainland northern Scotland)

08-DCOC-06, sampled at [NC 6887 6170]

The Druim Chuibhe Orthogneiss Complex comprises intermediate to felsic orthogneisses and amphibolites that are interbanded in approximately equal proportions on a scale of 3–5 m. The complex is *c.* 350 m thick and traceable laterally for 3 km (Fig. 3b). Contacts between the amphibolites and the intermediate to felsic orthogneisses are sharp and concordant. They form a bimodal igneous suite that appears to share a common structural and metamorphic history with host paragneisses (Burns 1994). The orthogneiss complex is underlain by the ductile Torrisdale Thrust (not considered to be of regional significance); its upper contact with paragneisses is concordant (Burns 1994; Strachan *et al.* 2010*a*). The sample is a fine- to medium-grained intermediate orthogneiss composed of hornblende, biotite, plagioclase, quartz, K-feldspar and garnet, with accessory titanite and zircon (Fig. 4g). The amphibolites are mostly medium grained and dominated by schistose layers of aligned hornblende ± biotite that wrap aggregates and individual grains of plagioclase and quartz. Titanite and ilmenite are common accessory minerals; garnet is rare to absent in most thin sections. Amphibolites and felsic orthogneisses from the complex were also sampled for chemistry.

Amphibolite intrusions within the Yell Sound Group

A number of amphibolite units from Yell and mainland Shetland were sampled for chemistry. The amphibolites typically occur as concordant sheets or boudins and vary from 0.5 to 2 m in thickness. Only one suite was observed: no examples were seen of one amphibolite cutting another. Most are medium- to coarse-grained and comprise hornblende, garnet, plagioclase and quartz with accessory opaque minerals and titanite. They contain little to no zircon. Minor petrological and textural differences arise from variations in Caledonian temperatures between *c.* 650°C and *c.* 750–800°C (Cutts *et al.* 2011). Amphibolites occur as parallel-sided, concordant sheets or boudins within the Gutcher, Breckon and Valayre granitic gneisses (Flinn 1994). This suggests that the amphibolites are younger than the igneous protoliths of the granitic gneisses. However, the Valayre granitic gneiss on Lunna Ness contains a prominent amphibolite xenolith (Fig. 4b; see above). Furthermore, in low-strain zones the Valayre granitic gneiss on Lunna Ness also contains occasional small, irregular-shaped inclusions of amphibolite within an often weakly foliated host (Fig. 4h). The resultant texture resembles the results of magma mixing, suggesting that the granitic and mafic protoliths were in part contemporaneous.

Analytical methods

Zircon U–Pb geochronology

Secondary ion mass spectrometry

This technique was used for all metapelite and orthogneiss samples except SH-07-08 (see below). Zircons were separated from crushed rock using standard magnetic and heavy liquid separation techniques. Selected grains chosen as far as possible to be representative of the whole population were mounted in epoxy resin with a selection of the following reference zircons (CZ3, BR266, OGC-1 and Temora-2). The grains were imaged using a cathodoluminescence (CL) detector fitted to a Phillips XL30 scanning electron microscope (SEM) using a 12 kV beam current. CL images were used to select analysis locations. U–Pb analyses were undertaken by sensitive high-resolution ion microprobe (SHRIMP) at the John de Laeter Centre, Curtin University, Perth, using the SHRIMP II ion microprobes. SHRIMP analyses were undertaken over several 24 h analytical sessions, in all cases using O_2^- as the primary ion beam, 2–5 nA primary current and Köhler illumination with aperture selection leading to analytical spot size of 20–30 μm diameter. Each spot analysis entailed a 15–20 min duty cycle, involving 6–7 cycles through the designated mass stations (i.e. reference Zr species, Pb isotopes, background, U, ThO and UO), following a preburn (60–120 s) to minimize any surface Pb, and with automatic centring on all major peaks. Analyses of reference zircon CZ3 ($^{206}Pb/^{238}U$ age 561.5 Ma, Nasdala *et al.* 2008) or BR266 (559 Ma, Stern 2001) were

used to calibrate measured Pb/U ratios of unknowns, and secondary reference standard OGC-1 (^{207}Pb/^{206}Pb age 3465 Ma, Stern *et al.* 2009) was used to monitor for Pb isotope fractionation. Data were processed using Squid (Ludwig 2009), and concordia diagrams were prepared using Isoplot (Ludwig 2003). Age uncertainties quoted in the text are 95% confidence. Analytical data are presented in Supplementary material 1.

Laser ablation inductively coupled plasma mass spectrometry

Sample SH-07-08 was crushed using a jaw crusher and disc mill and then sieved to <500 μm. Heavy mineral cuts were separated using a Wilfley table, then zircons were handpicked, mounted in epoxy resin and polished to half height. Grains were imaged using a Phillips XL30CP SEM and a CL detector at the University of Portsmouth. Zircon U–Pb analyses were carried by LA-ICP-MS at the University of Clermont Auvergne (Laboratoire Magmas et Volcans) using an Agilent 7500cs (quadrupole) ICP-MS instrument equipped with a dual system enhance sensitivity (Paquette *et al.* 2014) and a laser excimer 193 nm Resonetics Resolution M-50E. Each analysis consisted of *c.* 30 s background acquisition and 60 s sample acquisition. A 33 μm spot was used, with typical laser conditions of a 3 Hz repetition rate and a fluence of 4 J cm^{-2}. Ratios were calculated using standard–sample bracketing measuring GJ-1 zircon reference material (Jackson *et al.* 2004) as the primary standard and 91500 as secondary standard (Wiedenbeck *et al.* 1995). All uncertainties were propagated in quadrature. GJ-1 yielded a mean ^{206}Pb/^{238}U ratio of 0.09750 ± 0.00049 (2SD *n* = 29) and ^{207}Pb/^{206}Pb ratio of 0.06013 ± 0.00062 (2SD *n* = 29), whereas 91500 zircon standards yielded mean ^{206}Pb/^{238}U ages of 1067 ± 22 Ma (2SD; 1062.4 ± 0.4 Ma; Wiedenbeck *et al.* 1995) Data reduction was done using the software package GLITTER® (Macquarie Reseach Ltd; Van Achterbergh *et al.* 2001; Jackson *et al.* 2004). Calculated ratios were exported and concordia ages and diagrams were generated using the IsoplotR v.6.2.1 software package of Vermeesch (2018). Concentrations of U–Th–Pb were calibrated relative to GJ-1 value (Jackson *et al.* 2004). The amount of ^{204}Pb in these analyses was below background level, and therefore no common Pb correction was undertaken. All zircons of sufficient size were analysed, but only ages from a single growth zone and avoiding irregular features such as cracks and inclusions were used. Analytical data are presented in Supplementary material 2.

Zircon Hf isotope analysis

All Lu–Hf analyses were collected on zircon crystals previously analysed for U–Pb. For all samples except SH12-01 Burra Voe, Hf isotope analysis of zircon was carried out at the GeoHistory Facility, John de Laeter Centre, Curtin University using a Nu Plasma II multi-collector ICP-MS system attached to an excimer laser (RESOlution LE 193 nm ArF with a Lauren Technic S155 cell). A laser spot of 33 μm diameter was employed, with on-sample energy of *c.* 2.8 J cm^{-2}, repetition rate 10 Hz, 30 s analysis time, two cleaning pulses and 55 s background collection. Time-resolved data were baseline-subtracted and reduced using Iolite (data reduction scheme (DRS) after Woodhead *et al.* 2004). Data were normalized to ^{179}Hf/^{177}Hf = 0.7325 using an exponential mass fractionation function. Interference by ^{176}Lu on ^{176}Hf was corrected via ^{175}Lu, using ^{176}Lu/^{175}Lu = 0.02655; interference by ^{176}Yb on ^{176}Hf was corrected via ^{173}Yb, using ^{176}Yb/^{173}Yb = 0.7962 and applying a mass fractionation correction assuming ^{172}Yb/^{173}Yb = 1.35274 (Chu *et al.* 2002). The primary reference material used for monitoring the accuracy of Hf isotope ratios was the Mud Tank zircon (^{176}Hf/^{177}Hf = 0.282507 ± 0.000006, Woodhead and Hergt 2005); along with secondary reference zircons R33, FC-1, GJ-1,

Plešovice and 91500. For the Burra Voe sample, Hf analysis was undertaken at GEMOC, Macquarie University, Sydney using a New Wave/Merchantek Research LUV213 laser ablation microprobe, attached to a Nu Plasma multi-collector ICP-MS system. The 213 nm Nd:YAG laser was employed at a 5 Hz repetition with energies of 0.12–0.15 mJ per pulse, resulting in total signals of (1–6) × 10^{-11} A from 50 μm diameter pits. Ablation times of 200–250 s were used, with ablated material transported to the ICP-MS torch by a He carrier gas. Hf isotopes were measured simultaneously on Faraday cups in static-collection mode. The Burra Voe data were normalized to ^{179}Hf/^{177}Hf = 0.7325 using an exponential mass fractionation function. Interference by ^{176}Lu on ^{176}Hf was corrected using ^{176}Lu/^{175}Lu = 0.02669; interference by ^{176}Yb on ^{176}Hf was corrected via ^{172}Yb, using ^{176}Yb/^{172}Yb = 0.5865 (Griffin *et al.* 2000). Reference zircons Mud Tank and 91500 were analysed at intervals with the unknowns to monitor accuracy and precision of the corrected ^{176}Hf/^{177}Hf ratios. For all data, initial Hf, model ages and εHf values were calculated using the ^{176}Lu β^{-} decay constant of 1.865 × 10^{-11} (Scherer *et al.* 2001), Chondritic Uniform Reservoir (CHUR) parameters of Blichert-Toft and Albarède (1997) and Depleted Mantle (DM) parameters of Griffin *et al.* (2004). Two-stage T$_{DM}$ model ages assume an average ^{176}Lu/^{177}Hf of 0.015 for precursor crust (Griffin *et al.* 2004). Analytical data are presented in Supplementary material 3.

Major and trace element chemistry

Samples were split, passed through a jaw crusher and powdered in a tungsten carbide TEMA mill. Major elements and Sc, Cr, V, Cu, Zn, Ni, Rb, Sr, Y, Zr, Nb, Ba, Pb and Sn were analysed by X-ray fluorescence spectrometry, against calibrations defined with international certified reference materials (CRMs). Fusion discs were used for the major elements and pressed powder pellets for trace elements. REE, Hf, Ta, Th and U were analysed by ICP-MS following fusion dissolutions, also against calibrations defined with international CRMs. Accuracy and precision are monitored with independent CRMs and are estimated to be better than 1% for major elements and 5% for trace elements. Representative data are listed in Supplementary material 4.

Nd and Sr isotopes

Amphibolite samples were analysed for Nd and Sr isotopes at the NERC Isotope Geosciences Laboratory at Keyworth, Nottingham, UK. Samples were spiked with a mixed ^{149}Sm–^{150}Nd tracer and dissolved using HF–HNO$_3$. Sr and REE were separated using standard cation exchange methods, and Sm and Nd were then separated using Eichrom LN-SPEC ion exchange columns. Sr and Nd were analysed on a Thermo Scientific Triton mass spectrometer. Sr was loaded on single Re filaments using a TaO activator and analysed using a multidynamic algorithm. Nd was analysed using Ta–Re double filament assemblies, again using a multidynamic algorithm. Four analyses of the NBS987 standard run with the Sr samples gave a mean ^{87}Sr/^{86}Sr of 0.710254 ± 0.000002 (1σ). Three analyses of the La Jolla standard run with the Nd samples gave a mean ^{143}Nd/^{144}Nd of 0.511844 ± 0.000005. Analytical data are presented in Supplementary material Table 5.

Results and interpretation: U–Pb zircon geochronology and Hf isotopes

Yell Sound Group metapelites

S05/02 Brim Ness semi-pelitic gneiss

The heavy mineral concentrate from this sample yielded abundant brown zircon (and minor orange rutile). The zircons are typically
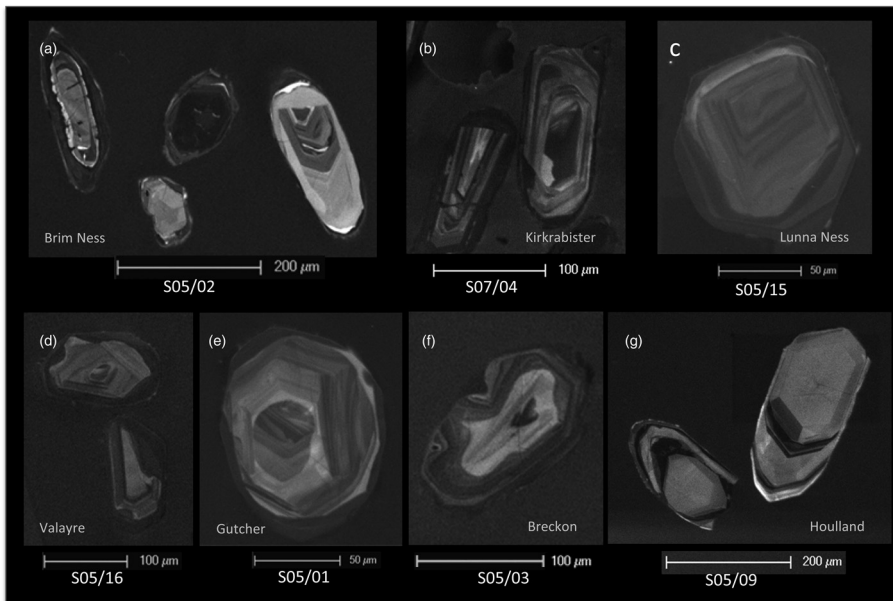
Fig. 5. CL images of representative zircons from samples (**a**) S05/02 (Brim Ness semi-pelitic gneiss), (**b**) S07/04 (Kirkrabister pelite), (**c**) S05/15 (Lunna Ness migmatitic gneiss), (**d**) S05/16 (Valayre granitic gneiss), (**e**) S05/01 (Gutcher granitic gneiss), (**f**) S05/03 (Breckon granitic gneiss) and (**g**) S05/09 (Houlland mafic orthogneiss).

subhedral, elongate prism shapes with bipyramidal terminations. CL images reveal regular internal magmatic zonation in most grains, some with embayed or modified internal zonation boundaries, and some with narrow, dark rims (Fig. 5a). SHRIMP spot analyses of 35 grain interiors define two broad age groups on the concordia diagram and age histogram (Fig. 6a): a dominant group with $^{207}Pb/^{206}Pb$ ages in the range 2550–2850 Ma, and a subordinate group with ages in the range 1700–1850 Ma. Additionally, one grain yielded a minimum apparent $^{207}Pb/^{206}Pb$ age of *c.* 3450 Ma. The presence of multiple age populations is consistent with the grains being a mixed detrital population derived from various Archean and Paleoproterozoic sources. Several grain rims were also analysed. These are characteristically low in Th, with Th/U < 0.10, and dark in CL. The analyses of these rims are generally among the most discordant analyses. Broadly, the discordance pattern is consistent with Paleozoic (Caledonian?) disturbance of a mixed population of inherited (detrital) Archean or Paleoproterozoic grains.

SH-07-04 Kirkrabister pelite

This sample contains small, prismatic, pink zircons with mostly regular internal zonation and dark (CL) rims (Fig. 5b). SHRIMP analyses of central areas within 20 grains produced a relatively even spread of near-concordant data points across the age range *c.* 1060–1820 Ma (Fig. 6b). Analyses of poorly luminescent, relatively

U-rich rims on seven grains yield discordant age data ranging in $^{207}Pb/^{206}Pb$ age from *c.* 880 Ma (minimum age for their formation) to *c.* 580 Ma. At *c.* 1060 Ma, the youngest concordant core age provides a maximum age constraint on deposition.

S05/15 Lunna Ness migmatitic gneiss

The heavy mineral concentrate from this sample is dominated by prismatic rutile (not analysed), with only minor zircon and monazite present. The zircons are small grains of very pale brown colour, occurring in a range of subhedral, equidimensional to somewhat elongate geometries. Larger, pale yellow monazite grains are tabular in shape. CL imaging and SIMS analysis of the zircons revealed zoned, luminescent cores (U < 500 ppm) surrounded by CL-dark rims (1000–2000 ppm U, Th/U < 0.02, Fig. 5c). On the concordia diagram, a group of eight cores form a concordant group with a mean $^{207}Pb/^{206}Pb$ age of 967 ± 15 Ma (analyses with blue shading, Fig. 7a). As the sample is interpreted as a metasediment, these are interpreted as the youngest detrital components. One core (in grain 11) is distinctly older at *c.* 1550 Ma. The remaining core analyses yield younger apparent ages than the main population (shaded grey, Fig. 7a). Together with the rim analyses (shown in red, Fig. 7b), they form a discordia line with calculated intercepts at 917 ± 29 and 475 ± 47 Ma (MSWD 2.2). The lower intercept age is similar to the 467 ± 4 Ma age obtained from monazite inclusions in garnet from this locality by LA-ICP-MS (Cutts
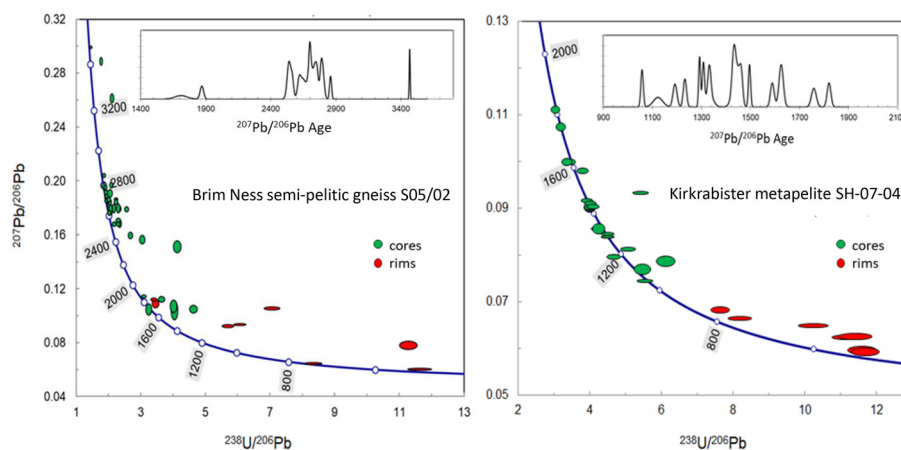

Fig. 6. Concordia plots and frequency distribution diagrams of SHRIMP zircon U–Pb data from (**a**) the Brim Ness semi-pelitic gneiss (S05/02) and (**b**) the Kirkrabister pelite (SH-07-04). Ages labelled on concordia are million years.
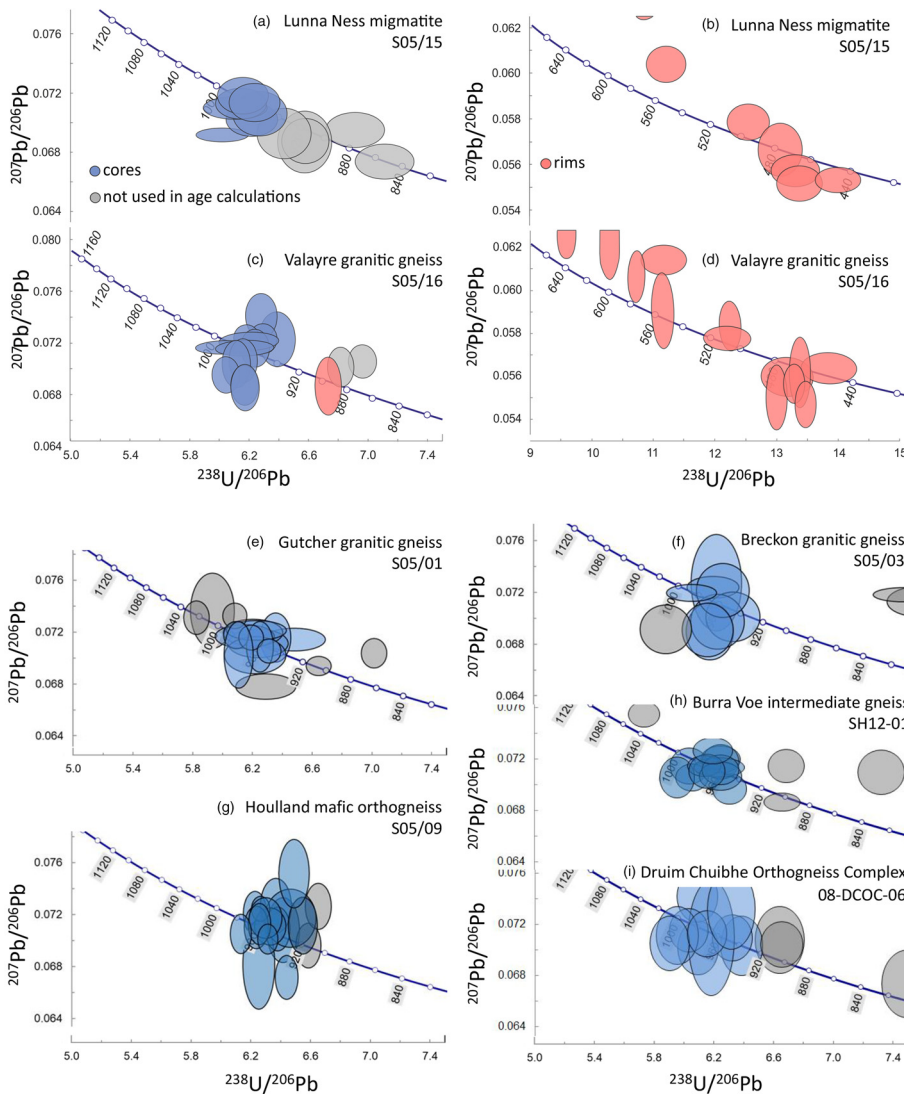
Fig. 7. Concordia plots of SHRIMP zircon U–Pb data: (**a**, **b**) Lunna Ness migmatite (SO5/15); (**c**, **d**) Valayre granitic gneiss (SO5/16); (**e**) Gutcher granitic gneiss (SO5/01); (**f**) Breckon granitic gneiss (SO5/03); (**g**) Houlland mafic orthogneiss (SO5/09); (**h**) Burra Voe intermediate gneiss (SH12/01); (**i**) Druim Chuibhe Orthogneiss Complex (08-DCOC-06). Ellipses show 1σ uncertainties of individual spot analyses. Data are given in Supplementary material 1. Analyses shaded blue denote magmatic zircon; red indicates zircon rims and/or recrystallized areas; grey denotes analyses not used in the age calculations for reasons of >5% discordance or possible inheritance or recrystallization. Ages labelled on concordia are million years.

et al. 2011). The distribution of data suggests that this sample experienced an early metamorphic episode (>c. 920 Ma) followed by an Ordovician overprint. Geothermobarometry on the metamorphic assemblage, presumably related to the overprint, indicates peak conditions of c. 10 kbar and 750–800°C (Cutts et al. 2011).

Felsic orthogneiss intrusions within the Yell Sound Group

S05/16 Valayre granitic gneiss

Except for a few rutile grains, the non-magnetic heavy mineral concentrate from this sample is close to 100% zircon. Externally, the zircons are pale brown in colour, glassy looking and widely ranging in shape and size. Most are euhedral or subhedral, and either equidimensional or with c-axis elongation up to 4:1. CL imaging revealed the presence of luminescent igneous-zoned cores in most grains, surrounded by a CL-dark rim. The cores, which are moderate in U content (<800 ppm), are often embayed and partially resorbed at the core–rim interface (Fig. 5d). The CL-dark rims are higher in U content (up to 2000 ppm) with low Th/U.

On the concordia diagram, a group of nine cores form a concordant group with a calculated mean ^{207}Pb/^{206}Pb age of 966 ± 7 Ma (Fig. 7c). No older cores were found, but several cores yield younger apparent ages suggesting partial Pb loss. Together with the analyses of rims (Fig. 7d), these points define a

discordance line (MSWD 2.0) with calculated concordia intercept ages of 953 ± 32 and 493 ± 46 Ma. Some of the rim analyses yield minimum ages as old as the disturbed cores, implying that the event that formed the rims occurred early in the post-crystallization history of the gneiss, potentially at c. 920 Ma, the age given by monazite inclusions in garnet from this locality by LA-ICP-MS (Cutts et al. 2011). We interpret the data from the concordant group of zircon cores to indicate that the igneous protolith was intruded at 966 ± 7 Ma.

Hf isotope analyses of 12 of the dated grains yield age-corrected εHf values (at t = 965 Ma) in the range −3.3 to −13.4. Such negative values (relative to CHUR) indicate a substantial crustal prehistory for the source rocks of the granitic magma that formed the Valayre granitic gneiss. The observed compositional range in Hf translates to two-stage T_{DM} model ages for the initial formation of the source rock(s) in the range 2.05–2.69 Ga.

S05/01 Gutcher granitic gneiss

This sample yielded abundant pale brown zircons, of widely ranging grain size and predominantly euhedral to subhedral prismatic shapes. CL imaging revealed regular magmatic zonation, with occasional internal embayments or truncations of zones, and commonly a dark (poorly luminescent) rim (Fig. 5e). The main population of SHRIMP analyses, shaded in blue in Figure 7e, plots as a cluster of 13 points overlapping the concordia curve with a

mean $^{207}Pb/^{206}Pb$ age of 965 ± 9 Ma. A few cores yield older apparent ages: one at *c.* 1200 Ma, two at *c.* 1570 Ma, two at *c.* 1800 Ma and one at *c.* 2720 Ma. Analyses of dark, relatively high-U rims with low Th/U yield a range of apparent ages: some points plot close to the main population, others yield younger apparent ages, with the youngest at *c.* 460 Ma ($^{206}Pb/^{238}U$ age, analysis 4.1).

These data suggest that the igneous protolith was intruded at *c.* 965 Ma, and inherited older grains from a mixed, presumably sedimentary precursor that contributed to the granitic melt. The dark rims probably represent either a late-stage magmatic or an early metamorphic overgrowth that variably lost radiogenic Pb at *c.* 460 Ma.

Hf isotope analyses of nine of the dated magmatic grains yield age-corrected εHf values (at $t = 965$ Ma) in the range -3.7 to -16.4. Given the U–Pb results outlined above, and that the U–Pb and Hf data were obtained separately, the most negative values could be due to the larger Hf analytical spot potentially incorporating an older inherited core. Two analyses specifically targeting older cores yield εHf values of -5.8 and -6.2 at $t = 1800$ Ma. The corresponding two-stage Hf T_{DM} model ages for both the magmatic and inherited zircon are in the range 2.07–2.88 Ga.

S05/03 Breckon granitic gneiss

Abundant, pale yellow–brown zircons were recovered from this sample. They are typically euhedral to subhedral, elongate grains. CL images revealed the presence of structural cores in some grains, and only very limited development of distinct rims (Fig. 5f). Twenty SHRIMP analyses were undertaken. The main population plots as a cluster of eight points overlapping the concordia curve with a mean $^{207}Pb/^{206}Pb$ age of 965 ± 11 Ma (Fig. 7f). A few analyses of cores yield older apparent ages: two at *c.* 1200 Ma, two at *c.* 1500 Ma, one at *c.* 1800 Ma and one at *c.* 2550 Ma. Several attempted analyses of outer parts of grains produced discordant age data with relatively young apparent ages but no clear age signature.

We interpret the data to indicate that the igneous protolith was intruded at *c.* 965 Ma, similar to the Gutcher granitic gneiss. Older apparent ages are interpreted to represent inherited (detrital) grains within a sedimentary precursor that contributed to the granitic melt. Although there are fewer analyses, the apparent ages are also consistent with those obtained from the Gutcher sample. The dark zircon rims are thought to represent late, high-U magmatic additions that variably lost Pb, rather than new growth at *c.* 460 Ma.

The results of Hf isotope analyses of zircons from the Breckon granitic gneiss are similar to the results from the Gutcher granitic gneiss. Six spots targeting *c.* 965 Ma magmatic zircon yield εHf$_{(t)}$ values in the range -2.1 to -12.2. Additionally, two inherited cores

yield εHf values of -3.6 ($t = 1800$ Ma) and $+4.1$ ($t = 2550$ Ma). Two-stage T_{DM} model ages are in the range 1.97–2.80 Ga, with the oldest model age coming from the *c.* 2550 Ma core.

Interbanded mafic to felsic orthogneiss within the Yell Sound and Sand Voe groups ('orthogneisses of uncertain affinity')

S05/09 Houlland mafic orthogneiss

The heavy mineral separate from this sample is dominated by titanite. Zircon occurs as small, subhedral, subrounded grains, pale brown in colour. In CL images (Fig. 5g), the grains show various combinations of sector and oscillatory zoning, often with partly resorbed cores. All of the analysed zircon grains are exceedingly low in Th content, generally <1 ppm with Th/U ratios averaging 0.002. Such low ratios are often characteristic of metamorphic zircon. Fifteen U–Pb analyses combine to a mean $^{207}Pb/^{206}Pb$ age of 951 ± 8 Ma (MSWD 3.0) (Fig. 7g). The three analyses with the lowest $^{206}Pb/^{238}U$ ratio (analyses 1a, 8a and 17; Supplementary material Table 1) were omitted from the calculation. Our preferred interpretation is that these represent the crystallization age of the magmatic protolith but the possibility that they relate to the time of zircon growth during amphibolite-facies metamorphism cannot be ruled out. The Hf isotopic composition of the grains is unusually radiogenic for their indicated age, plotting on or above the Depleted Mantle reference line (Fig. 8). The reason is most probably some systematic error in the Yb correction, affecting data that are already strongly radiogenic. εHf values (for $t = 950$ Ma) range from $+14.4$ to $+18.0$.

SH12-01 Burra Voe felsic orthogneiss

Zircons in this sample are mainly pale yellow, 100–200 μm in size, and euhedral to subhedral. CL images show brightly luminescent, oscillatory-zoned igneous cores in about half of the grains, the others having darker, unzoned cores. Thin CL-bright discontinuous rims are observed on some grains. Nineteen zircon cores and overgrowth domains were analysed, of which 15 are <10% discordant. The concordant grains yield a weighted mean $^{207}Pb/^{206}Pb$ age of 966 ± 11 Ma interpreted as the time of crystallization of the magmatic protolith (Fig. 7h). Hf isotopic analyses were carried out on nine selected zircon grains. Eight of these yield a narrow range of initial $^{176}Hf/^{177}Hf$ compositions at 965 Ma, corresponding to εHf values ranging from $+0.8$ to $+3.4$ (Fig. 8). The ninth analysis yields a distinctly less radiogenic Hf composition, with εHf of -16.2 (Fig. 8), indicating the likely incorporation of older inherited zircon into this analysis.
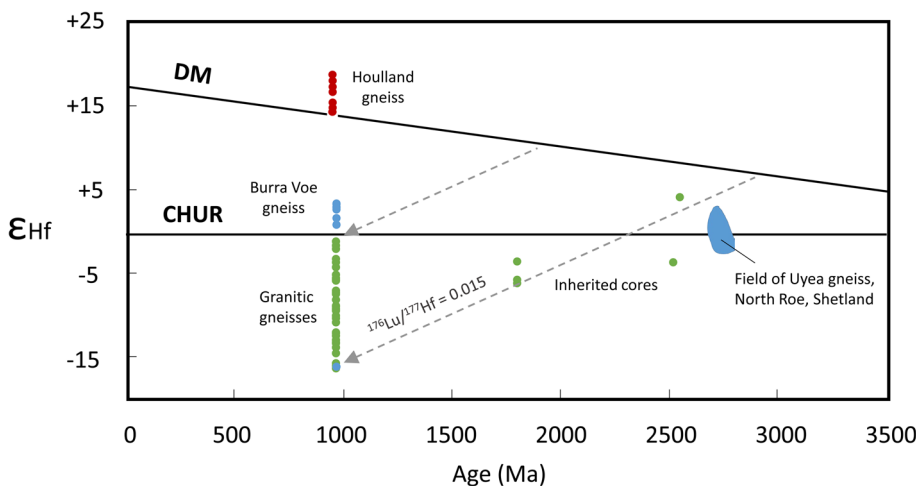

Fig. 8. Hafnium isotope evolution diagram. Representative individual analyses of zircons are shown as green dots (granitic gneisses), blue and red dots (Burra Voe and Houlland felsic–mafic orthogneisses respectively). Also shown is the field occupied by hafnium data obtained from the Neoarchean Uyea Gneiss Complex of NW Shetland (Kinny *et al.* 2019).
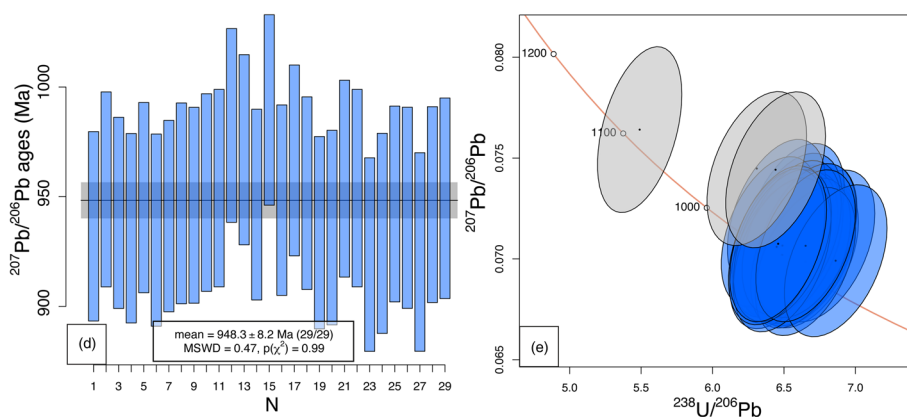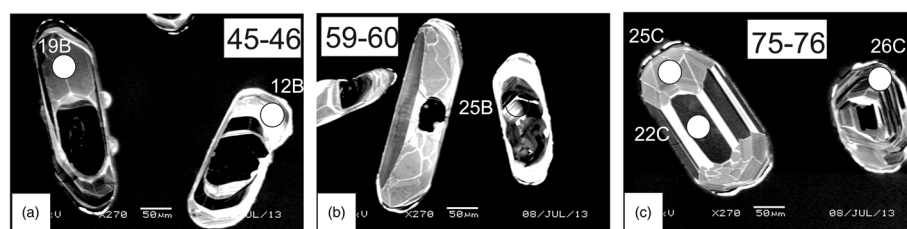
Fig. 9. (**a**–**c**) CL images of representative zircons from the Kirkaby felsic orthogneiss sample SH-07-08, with oscillatory and sector zoned crystals. (**d**) Mean $^{207}Pb/^{206}Pb$ ages obtained from the entire set of data except the single measured xenocryst and the two other grains with older ages visible in (**e**). (**e**) Concordia diagram with the entire dataset. Analyses shaded blue denote magmatic zircon; those shaded grey represent discordant (>7%) or xenocryst data.

Interbanded mafic and felsic orthogneiss within the Westing Group

SH07-08 Kirkaby felsic orthogneiss

Zircons grains mostly ranged between 200 and 300 μm in size. Crystals exhibit well-developed sector and oscillatory zoning (Fig. 9a–c) and some have xenocryst cores that are often heavily altered. Two analyses yield older apparent ages at *c.* 1050 Ma and one xenocryst an age of *c.* 1106 Ma (Fig. 9e and Supplementary material Table 2). For all other zircons analysed in this sample, no relationship between core v. rim, or oscillatory v. sector zoning and age can be established. Results obtained on these zircons are all within uncertainties of each other (Fig. 9d) and yield a mean $^{207}Pb/^{206}Pb$ age of 948.3 ± 8.2 Ma (95% confidence; $n = 29$; MSWD = 0.47), which is interpreted as the crystallization age of the magmatic protolith.

Intermediate orthogneiss within the Naver nappe, mainland northern Scotland

08-DCOC-06, Druim Chuibhe Orthogneiss Complex

Zircons from this sample are an assortment of pale yellow–brown, sub-rounded grains varying in shape from equant to highly elongate forms. All mounted grains luminesced strongly under CL. Generally, the grains display sectors of regular internal zonation, but often truncated against irregular-shaped or modified internal boundaries. On the concordia diagram, a group of eight cores form a coherent age group with a mean $^{207}Pb/^{206}Pb$ age of 958 ± 15 Ma (MSWD 0.47, Fig. 7i), which is interpreted as the magmatic intrusion age of the complex. This provides a minimum age constraint on the deposition of the host metasedimentary rocks. In addition, there are numerous analyses, including some identifiable as of structural cores, that yield ages in the range 1300–1750 Ma, and one discordant analysis with a minimum $^{207}Pb/^{206}Pb$ age of *c.* 2530 Ma. Narrow, dark rims or outgrowths are a feature of some grains. SHRIMP analyses of two of these domains showed them to have low Th/U (*c.* 0.01) and to be approximately concordant with a mean $^{206}Pb/^{238}U$ age of 461 ± 9 Ma, consistent with their formation during Grampian metamorphism.

Hf isotopic analyses were carried out on 11 selected zircon grains. Ten of these, which targeted magmatic zircon, yield initial εHf values ($t = 965$ Ma) ranging from -1.2 to -16.1. Given that the U–Pb and Hf data were obtained separately, the most negative values could be due to the larger Hf analytical spot potentially incorporating older inherited material. The eleventh analysis, specifically targeting the ≥2530 Ma inherited core, yields an even less radiogenic Hf composition, with $\varepsilon Hf_{(t)}$ of -3.5. The two-stage T_{DM} model age calculated for this analysis was 3.27 Ga, compared with model ages of 1.91–2.85 Ga for the magmatic zircons.

Results and interpretation: amphibolite and mafic orthogneiss chemistry and Nd–Sr isotopes

Although the chemistry of mafic igneous rocks is a common route to palaeotectonic interpretation, care must be taken to consider the possible effects of element mobility during metamorphism. This is often evident in the concentrations and relationships of fluid-mobile elements such as those of the large ion lithophile group (LILE), which includes Na and K, Rb, Sr and Ba. Consequently, interpretations are often based on the abundances of relatively immobile trace elements such as the REE and high field strength elements (HFSE) such as Zr, Hf, Nb, Ta and Th. Discrimination diagrams designed on the basis of these elements are widely used in the literature, constructed with data from young rocks of known tectonic settings. The amphibolites and mafic orthogneisses analysed have a rather uniform chemistry, varying on a theme of gabbro and apparently controlled by likely magmatic processes. This lends confidence to their use as indicators of Neoproterozoic tectonic setting, as it suggests that only modest metamorphic element redistribution has occurred.

Major element variations are shown in Figures 10 and 11. The amphibolites and mafic orthogneisses are all classified as gabbro to gabbro–diorite on the plutonic total alkali–silica diagram (Fig. 10a). On an AFM diagram (Fig. 10b) all data plot in the tholeiitic field. A selection of variation plots against MgO is presented in Figure 11a–h, demonstrating coherent arrays of data in the Shetland samples for Al_2O_3, FeO*, CaO, TiO_2 and P_2O_5 across an MgO range of 4–11 wt %. SiO_2, Na_2O and K_2O are rather more scattered by comparison, possibly the result of metamorphic redistribution as noted above.
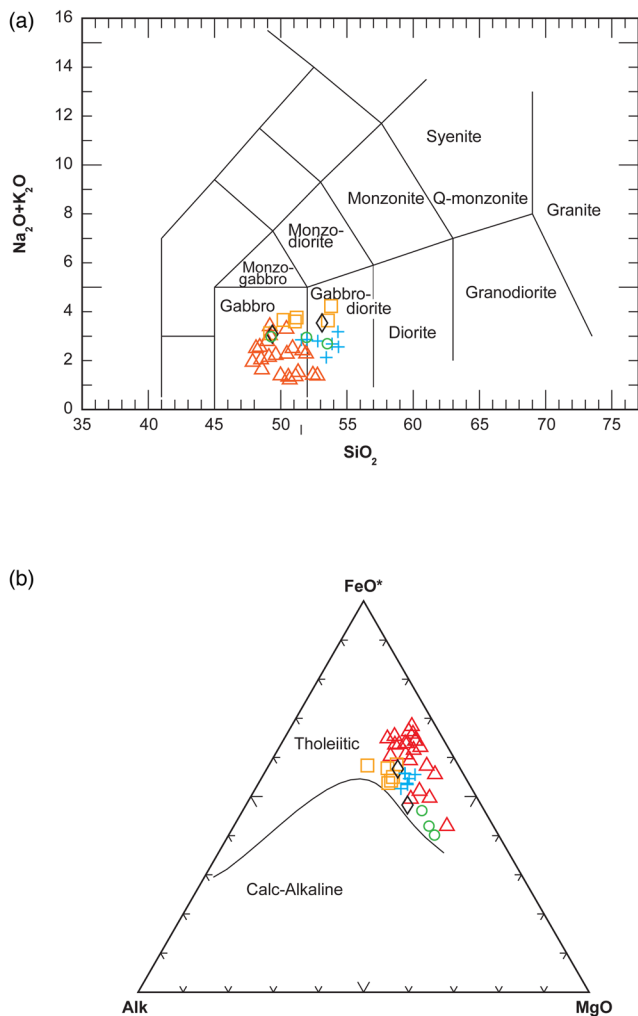
Fig. 10. Petrological affinities of Yell Sound and Druim Chuibhe amphibolites and mafic orthogneisses: (**a**) chemical assignment of protolith; (**b**) AFM diagram showing tholeiitic–calc-alkaline divide. Red triangles, Yell Sound amphibolites; orange squares, Druim Chuibhe amphibolites; blue crosses, Kirkaby orthogneiss; green circles, Burra Voe orthogneiss; black diamonds, Houland Quarry orthogneiss.

The DCOC samples overlap the Shetland data in SiO_2, CaO, Na_2O and P_2O_5, but plot in largely separate fields for Al_2O_3, FeO*, TiO_2 and K_2O. They show no significant trends with decreasing MgO.

Trace element variations are illustrated as mantle-normalized patterns in Figure 12a–c. Figure 12a represents the Yell Sound Group amphibolites, in which some variation is indicated by positive and negative Sr anomalies (and Eu anomalies on full chondrite-normalized REE patterns, not shown). Figure 12b displays data obtained from the Houlland, Burra Voe and Kirkaby mafic orthogneisses. Figure 12c displays the amphibolite samples from the Druim Chuibhe Orthogneiss Complex for comparison. All rocks show a rather flat section from Lu to P, a large peak at Pb, a general left-upward trend from Ce to Rb with troughs at Nb and Ba and peaks at Th and sometimes K. The Shetland samples with negative Sr and Eu anomalies have rather higher Lu–P in general than those with small peaks at Sr and Eu. On the major element diagrams the former have relatively low CaO and Al_2O_3 but high Fe_2O_3, TiO_2 and P_2O_5. The Druim Chuibhe Orthogneiss Complex samples show an overall close comparability with the low-Sr and -Eu group from Shetland.

The major element variations within the Shetland suite, and the accompanying Sr and Eu anomalies associated with higher or lower Lu–P can be interpreted in terms of minor plagioclase fractionation

in a basaltic magma: accumulation in those with high Sr, Eu, Al_2O_3 and CaO and removal from those with complementary characteristics. The overall shape of the mantle-normalized trace element plots is similar to that for subduction-related magmas, with negative Nb–Ta anomalies and enrichment in LILE likely to be mobile in the subduction environment (but note that LILE are also likely to be mobile during metamorphism). To pursue this possibility, a number of palaeotectonic discrimination diagrams are shown in Figure 13a–c, avoiding the LILE. In each of these, the amphibolites and mafic gneisses plot largely within the arc basalts or island-arc fields. It is therefore reasonable to conclude that the parent basalts were probably generated in a subduction-related environment.

A selection of the Yell Sound Group amphibolites was also analysed for Nd and Sr isotopes. Data are shown on an Nd isotope evolution diagram (Fig. 14). Estimated initial Sr isotope ratios vary between 0.6884 and 0.7156. The former is geologically unrealistic, even at *c.* 1000 Ma. Because both parent and daughter nuclides are LILE and therefore likely to be mobile during metamorphism, these are likely to be unreliable indicators of petrogenesis. The εNd data cluster between +3.6 and −0.4, with an outlier at −5.2. As REE are notably less mobile, Nd isotopes are more robust indicators of magma origin. The Yell Sound Group amphibolites with positive Eu and Sr anomalies have relatively high Sm/Nd, consistent εNd values of 2.7–3.6 at 960 Ma, and two-stage depleted mantle model ages (DePaolo *et al.* 1991) between 1255 and 1335 Ma (Fig. 14). Samples with negative Eu and Sr anomalies have lower Sm/Nd, εNd_{960} between −0.4 and 2.0, and model ages between 1395 and 1595 Ma. The slightly lower εNd and older model ages shown by the samples with negative Eu and Sr anomalies may reflect heterogeneity in the source region; alternatively, these samples may have assimilated small amounts of crustal material. One sample (A0603) has an unusual LREE pattern with a La kick and small negative Ce anomaly. This sample has a high initial Sr ratio at 960 Ma, together with a low εNd value of −5.2, and a relatively old model age of 1947 Ma. The most likely explanation is that sample A0603 has assimilated significant quantities of older crust.

Discussion

Constraints on depositional ages and potential source regions

The depositional ages of the Yell Sound Group and the metasedimentary rocks of the Naver Nappe are bracketed by the ages of the youngest inherited (detrital) zircon grains and the oldest intrusions in each succession. In the case of the Yell Sound Group samples, the youngest group of inherited zircon grains from the Kirkrabister (SH-07-04) pelite is *c.* 1.05–1.2 Ga, which provides a potential lower age limit on deposition. However, if the concordant group of eight zircon cores that yielded an age of 967 ± 15 Ma in the Lunna Ness migmatitic gneiss (S05/15) is detrital as we suggest, then deposition may have continued until, and potentially after, the intrusion of the igneous protoliths of Valayre, Gutcher and Breckon granitic gneisses at *c.* 965 Ma. The apparently detrital zircon grains from the Lunna Ness migmatitic pelites could have been eroded from the extrusive equivalents of the felsic intrusions. In the case of the Naver Nappe, deposition occurred after the age of the youngest inherited zircon grain (1005 ± 18 Ma; Kinny *et al.* 1999) but prior to intrusion of the Druim Chuibhe Orthogneiss Complex (*c.* 960 Ma). Both successions were therefore deposited at approximately the same time.

The numbers of analyses are relatively small, but the ages of the inherited zircon grains can potentially be used to constrain likely source areas for the two sedimentary successions. Taking the analyses from the Brim Ness (S05/02) and Kirkrabister (SH-07-04)
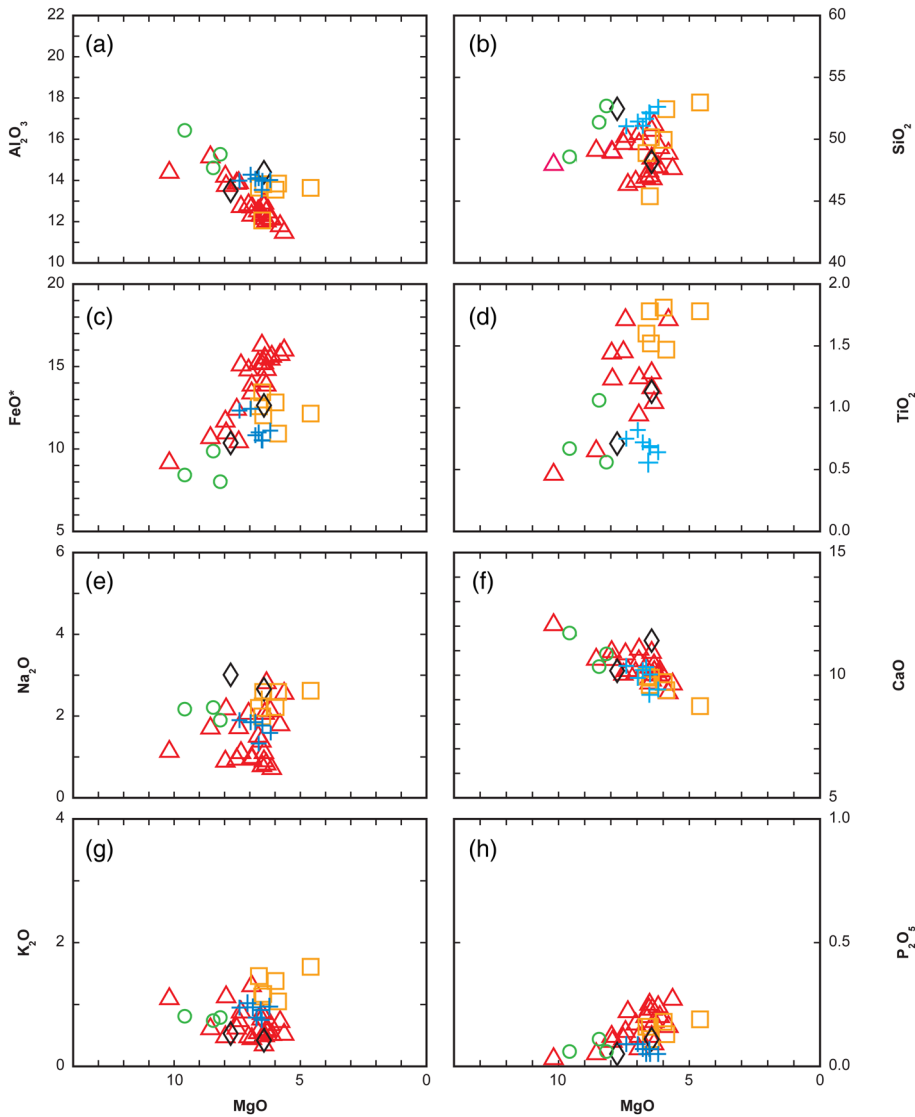
Fig. 11. (a–h) Major element variations in Yell Sound and Druim Chuibhe amphibolites and mafic orthogneisses, plotted against MgO as a fractionation index. Red triangles, Yell Sound amphibolites; orange squares, Druim Chuibhe amphibolites; blue crosses, Kirkaby orthogneiss; green circles, Burra Voe orthogneiss; black diamonds, Houland Quarry orthogneiss.

metapelites as a whole, there are broad age clusters at 2.8–2.5, 1.85–1.75, 1.6, 1.5–1.4, 1.3 and 1.2–1.05 Ga (Fig. 6). These are consistent with more comprehensive datasets obtained from various other Tonian sedimentary successions deposited on the margin of eastern Laurentia (Cawood *et al.* 2007, 2015; Kirkland *et al.* 2008*b*; Olierook *et al.* 2020). In all cases, derivation of detrital zircons from eastern Laurentia has been invoked to explain the main age clusters, although unambiguous distinction between Laurentian and Baltican sources is difficult (e.g. Slagstad and Kirkland 2017). Hence both areas record tectonic events that correspond to three of the main age clusters from the new data reported here: (1) Neoarchean accretion of cratonic nuclei (2.8–2.5 Ga); (2) punctuated convergent margin tectonism along the eastern and southern margins of Laurentia and Baltica (1.85–1.7 Ga); (3) Grenvillian and Sveconorwegian orogenesis (1.2–1.05 Ga). However, it is noted that Paleoarchean crust that would correspond to the single 3.45 Ga grain is relatively rare in Baltica and such detritus is more probably derived from West Greenland or eastern Labrador (Nain province) (Cawood *et al.* 2007).

Age and tectonic setting of Tonian magmatism

The U–Pb zircon ages of *c.* 970–950 Ma reported here for a range of mafic, intermediate and felsic meta-igneous rocks in the Shetland Islands and northern Scotland represent the first evidence for Tonian magmatism in this sector of the North Atlantic borderlands. The Houlland and Burra Voe orthogneisses are interpreted as part of this magmatic suite and there is no field, geochemical or isotopic evidence that they are infolds or tectonic slices of an older 'Lewisianoid' basement (Flinn 1988, 1994). The palaeotectonic discrimination diagrams (Fig. 13) all suggest that the protoliths of the Yell Sound Group and Druim Chuibhe amphibolites and the Houlland, Burra Voe and Kirkaby mafic orthogneisses were emplaced in a subduction-related setting. The Hf isotope data for the dated Houlland and Burra Voe samples, as well as the εNd isotope data for the amphibolites, indicate that these represent relatively juvenile crustal contributions. The range of inherited zircons within the felsic orthogneiss intrusions is similar to that of their host gneisses. This reinforces the suggestions from the chemistry of these rocks that they are crustal melts (Supplementary material File 6) and their chemistry is therefore less likely to be a reliable indicator of tectonic environment. Generation of the protoliths of the felsic orthogneisses may have resulted from the advection of heat and crustal melting consequent on intrusion of the precursors of the amphibolites and the mafic gneisses.

Ages of regional metamorphic events

Although not well constrained, the Lunna Ness migmatitic pelite (S05-15) within the Yell Sound Group records two phases of zircon growth, which are interpreted as corresponding to regionally
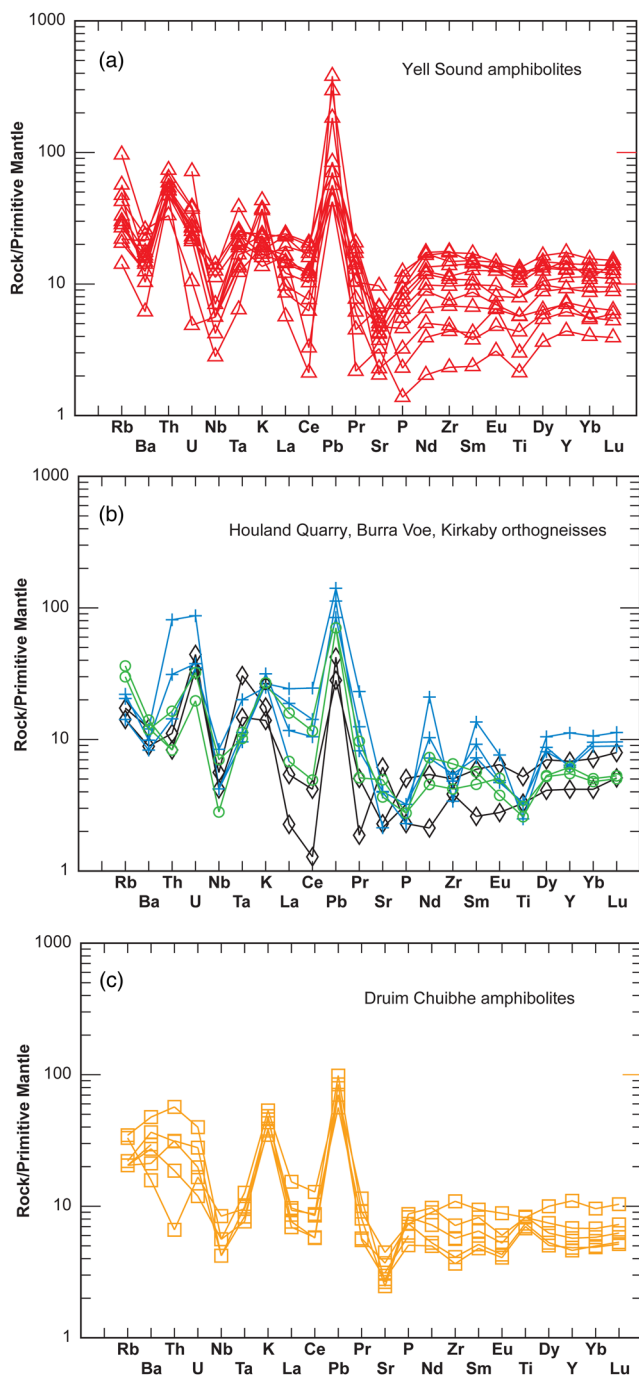
Sound Group (and associated granitic gneisses) was affected by amphibolite-facies metamorphism at *c.* 940–920 Ma.

Younger, Ordovician, metamorphism at 475 ± 47 Ma corresponds to the early Caledonian Grampian orogenic event widely recognized in Scotland and Ireland and broadly correlative with the Taconic event in the Appalachians (e.g. Lambert and McKerrow 1976; Dewey and Shackleton 1984; Dewey and Ryan 1990; Van Staal *et al.* 1998, 2009; Friedrich *et al.* 1999; Oliver *et al.* 2000; Baxter *et al.* 2002; Chew *et al.* 2003, 2008, 2010). This resulted from the collision of the Laurentian passive margin with an intra-oceanic arc at an early stage in the closure of the Iapetus Ocean. Obduction of ophiolites (e.g. Unst ophiolite, Fig. 2b) onto the Laurentian margin was followed by regional deformation and
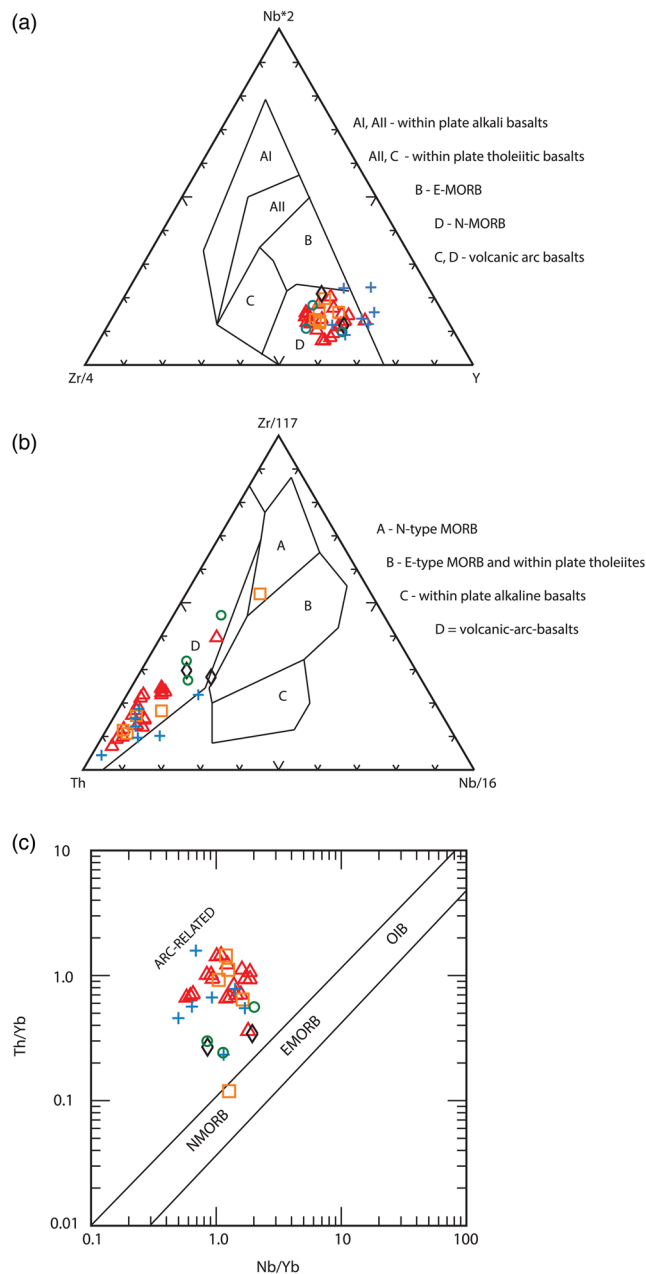

Fig. 12. (**a**–**c**) Petrogenetic trace element characteristics of Yell Sound and Druim Chuibhe amphibolites and mafic orthogneisses, normalized to primitive mantle abundances. Red triangles, Yell Sound amphibolites; orange squares, Druim Chuibhe amphibolites; blue crosses, Kirkaby orthogneiss; green circles, Burra Voe orthogneiss; black diamonds, Houland Quarry orthogneiss. Source: Sun and McDonough (1989).

Fig. 13. (**a**–**c**) 'Immobile' trace element discrimination diagrams for Yell Sound and Druim Chuibhe amphibolites and mafic orthogneisses. Red triangles, Yell Sound amphibolites; orange squares, Druim Chuibhe amphibolites; blue crosses, Kirkaby orthogneiss; green circles, Burra Voe orthogneiss; black diamonds, Houland Quarry orthogneiss. E-MORB, enriched mid-ocean ridge basalt; N-MORB, normal MORB; OIB, ocean ridge basalt. Source: (a) after Wood (1980); (b) after Meschede (1986); (c) after Pearce (2008).
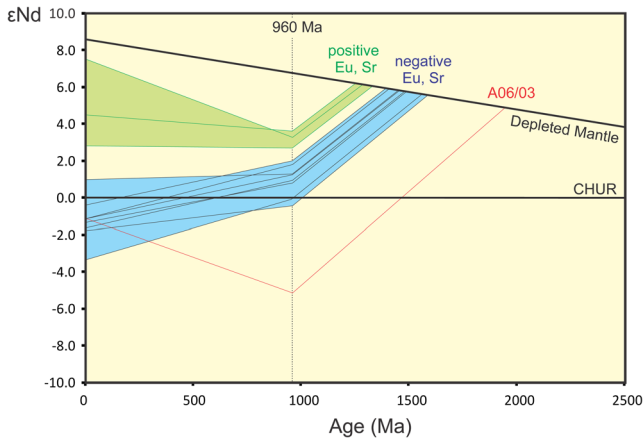
significant metamorphic events. The older at 917 ± 29 Ma is similar to the *c.* 944–931 Ma upper amphibolite- to granulite-facies metamorphic event identified previously within the Yell Sound Group (Jahn *et al.* 2017) and the *c.* 938–925 Ma upper amphibolite-facies metamorphic event reported from the Westing Group (Cutts *et al.* 2009*b*). The latter occurred at peak conditions of *c.* 650–700°C and 7 kbar and resulted in migmatization. Monazite grains from a sample of the Valayre granitic gneiss fall on a discordia between *c.* 460 and *c.* 920 Ma, with most of the older ages originating from monazite grains shielded within garnet grains (Cutts *et al.* 2011). This reinforces our interpretation that the Yell

Fig. 14. Nd isotope evolution diagram, illustrating the range of εNd values shown by Yell Sound Group amphibolites at 960 Ma, together with two-stage depleted mantle model ages. Source: DePaolo et al. (1991).

Barrovian metamorphism of footwall sedimentary successions. In Shetland, Lu–Hf and Sm–Nd garnet ages from samples of the Yell Sound Group and the East Mainland Succession that vary between 485 and 466 Ma probably correspond to the metamorphic peak (Walker et al. 2021). $^{206}Pb/^{238}U$ monazite ages between 462 and 451 Ma probably reflect cooling and exhumation (Cutts et al. 2011). Within the Druim Chuibhe Orthogneiss Complex of the Naver Nappe, the average age of 461 ± 9 Ma obtained from the rims of two zircon grains is also interpreted as corresponding to Grampian metamorphism, previously constrained to have occurred at c. 470–460 Ma (Kinny et al. 1999). The amphibolites of the complex contain relic clinopyroxene and garnet assemblages formed during peak metamorphism, and the new data presented here are consistent with the Ordovician (Grampian) age proposed for this event by Friend et al. (2000).

Correlations with other circum-North Atlantic successions

The Yell Sound and Westing groups and the metasedimentary rocks of the Naver Nappe can be correlated with the oldest of three broad lithotectonic groupings or megasequences each of which accumulated on, or proximal to, NE Laurentia in the Neoproterozoic (Cawood et al. 2007; Kirkland et al. 2008b; Olierook et al. 2020; Fig. 15). The oldest, 'megasequence 1', comprises successions deposited around or shortly after c. 1000 Ma, constrained in most

cases by the ages of the youngest detrital zircons that they contain and of the oldest igneous intrusions. However, their subsequent tectonomagmatic records show significant variations, presumably the result of their differing locations relative to zones of active deformation and/or melt generation. Thus, in the Caledonides of mainland Scotland the Morar Group does not contain any evidence for post-1000 Ma magmatism but was metamorphosed at c. 940–930 Ma (Bird et al. 2018). Further west, the Sleat and Torridon groups on the Hebridean foreland are thought to be laterally equivalent to the Morar Group (Krabbendam et al. 2008, 2017, 2021; Bonsor et al. 2012) but contain no evidence for Neoproterozoic igneous activity, deformation or metamorphism. Other 'megasequence 1' successions of NE Laurentia (Fig. 15) occur within the Pearya terrane of Ellesmere Island (Malone et al. 2014, 2017) and NW, SW and East Svalbard (Johansson et al. 1999, 2004, 2005; Pettersson et al. 2009; Majka et al. 2014). All of these sequences contain evidence for c. 980–960 Ma felsic magmatism that overlaps with the magmatic record documented here from Shetland and northern mainland Scotland (Fig. 16), although the timing of early deformation and metamorphism is uncertain in some cases. In contrast, the Krummedal Succession of East Greenland was deformed and metamorphosed at c. 950–930 Ma (Strachan et al. 1995; Watt and Thrane 2001), and underwent widespread anatexis resulting in the production of crustally derived granites, the youngest of which were emplaced at c. 915 Ma (Leslie and Nutman 2003; Fig. 16). Laurentian-derived correlatives of megasequences 1 and 2 are also present in north Norway, where they were tectonically emplaced as the Kalak Nappe Complex during the Caledonian orogeny (Fig. 15; Kirkland et al. 2006, 2007).

Implications for Rodinia reconstructions and plate-tectonic models

The evidence for 970–950 Ma calc-alkaline magmatism in Pearya (Malone et al. 2014, 2017), Svalbard (Johansson et al. 1999, 2004, 2005; Pettersson et al. 2009), and Shetland and mainland northern Scotland (this study) is consistent with the existence of an early Tonian subduction zone that dipped beneath the margin of NE Laurentia (Fig. 17). However, continental reconstructions differ in respect of whether the Scotland–Greenland segment underwent collisional orogenesis with Baltica in the early Tonian (Fig. 17a) or was bordered by an accretionary orogen through the Neoproterozoic (Fig. 17b and c).

Lorenz et al. (2012) and Gee et al. (2015) envisaged that the 'megasequence 1' successions of NE Laurentia accumulated within
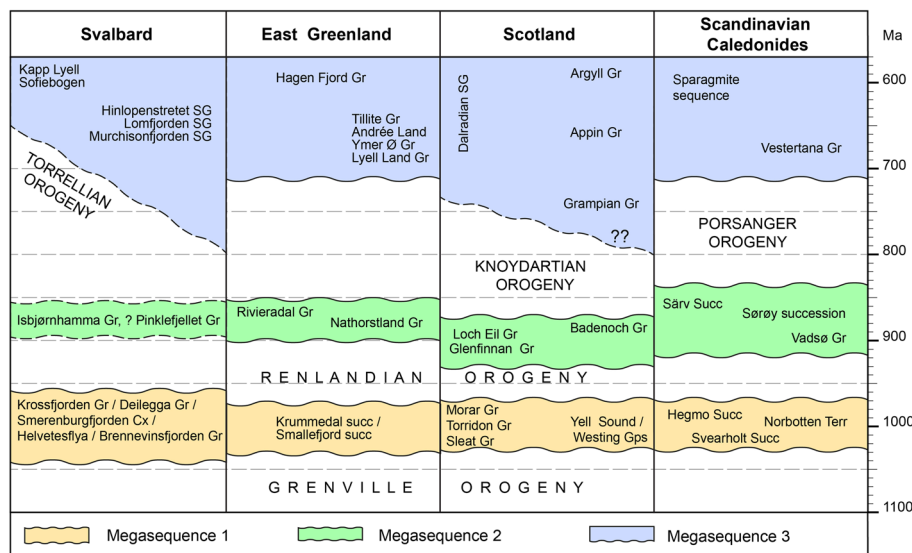

Fig. 15. Overview of Mesoproterozoic and Neoproterozoic megasequences in the North Atlantic region. Within each column, the horizontal placings of stratigraphic units reflect differing geographical or tectonic settings. SG, supergroup; Gr, group; Gps, groups; Cx, complex; Succ, succession; Terr, terrane. Source: Olierook et al. (2020); Strachan et al. (2024b).
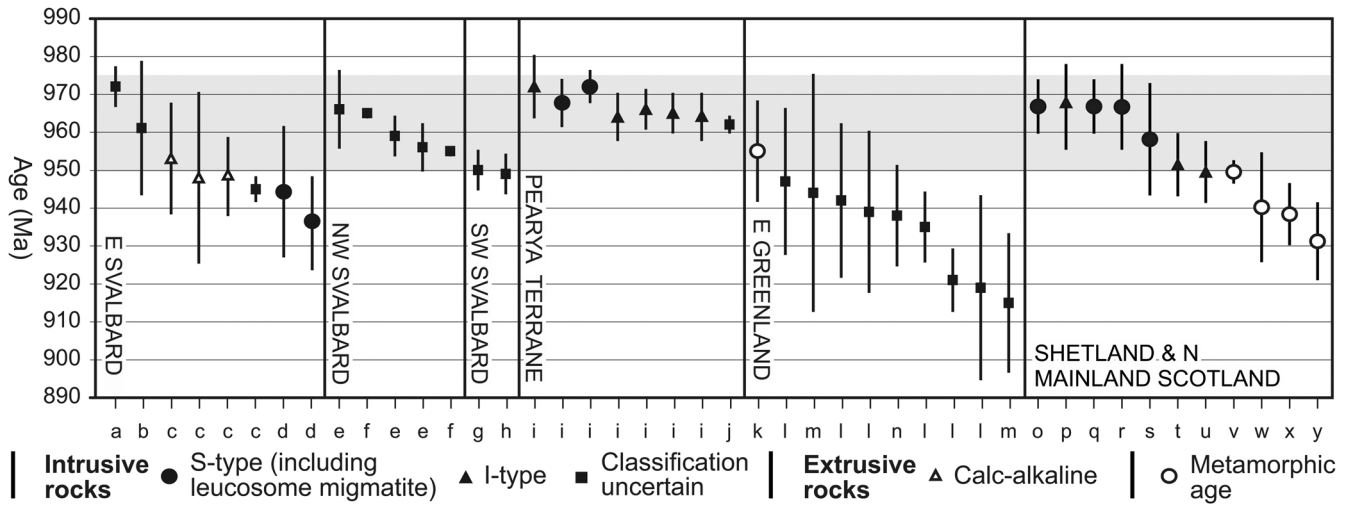
Fig. 16. Summary of U–Pb zircon ages derived from concordant analyses of Tonian meta-igneous rocks from Svalbard, the Pearya terrane of Ellesmere Island and East Greenland (McClelland *et al.* 2018), to which have been added data from the present study. The datasets for East Greenland and Shetland include U–Pb ages obtained from analyses of concordant zircon grains thought to have formed during regional metamorphism, as well as a Lu–Hf garnet age obtained from the Morar Group in northern mainland Scotland (age 'v'). The I- and S-type affinities of the Shetland and Naver Nappe meta-igneous rocks were established by plotting analyses of major elements on ternary discrimination diagrams (see Supplementary material Fig. S1 and accompanying text). The grey box emphasizes the similar timing of Tonian magmatism in Svalbard, Pearya, Shetland and the Naver Nappe. Data source: a, McClelland *et al.* (2018); b, Gee *et al.* (1995); c, Johansson *et al.* (1999); d, Johansson *et al.* (2004); e, Pettersson *et al.* (2009); f, Peucat *et al.* (1989); g, Majka *et al.* (2014); h, Gasser and Andresen (2013); i, Malone *et al.* (2017); j, Trettin *et al.* (1992); k, Strachan *et al.* (1995); l, Kalsbeek *et al.* (2000); m, Leslie and Nutman (2003); n, Watt *et al.* (2000); o, this study, Valayre granitic gneiss; p, this study, Burra Voe intermediate orthogneiss; q, this study, Gutcher granitic gneiss; r, this study, Breckon granitic gneiss; s, this study, Druim Chuibhe Orthogneiss Complex; t, this study, Houlland mafic orthogneiss; u, this study, Kirkaby mafic orthogneiss; v, Bird *et al.* (2018); w, Jahn *et al.* (2017); x, y, Cutts *et al.* (2009b).

a series of foreland or successor basins developed along the periphery of a collisional third arm of the Grenvillian–Sveconorwegian orogenic system (Fig. 17a; see also Park 1992 and Strachan *et al.* 1995, who considered a 'delayed collision' model). According to this interpretation, *c.* 950–920 Ma Renlandian orogenesis represented the final stages of Laurentia–Baltica collision. In this reconstruction, East Greenland and west Baltica would have formed opposing continental margins during the subsequent break-up of this segment of Rodinia in the Ediacaran, and some commonality in the nature and timing of passive margin basin development might be expected. However, the thick (up to

16 km), uniformly shallow-water Tonian to Ordovician successions of East Greenland and Svalbard contrast with the rather thinner (5–6 km), shallow- to deep-water and younger Cryogenian to Cambrian–Ordovician successions of Baltica (Nystuen *et al.* 2008). Furthermore, there is no evidence that basin development on the Laurentian side was accompanied by any magmatism, whereas the Baltica margin hosts an 800 km long segment of crust that was intruded by voluminous mafic dykes at *c.* 610–595 Ma (Abdelmalak *et al.* 2015). These contrasts argue against Rodinia reconstructions that place the Scotland–Greenland segment of NE Laurentia opposite Baltica.
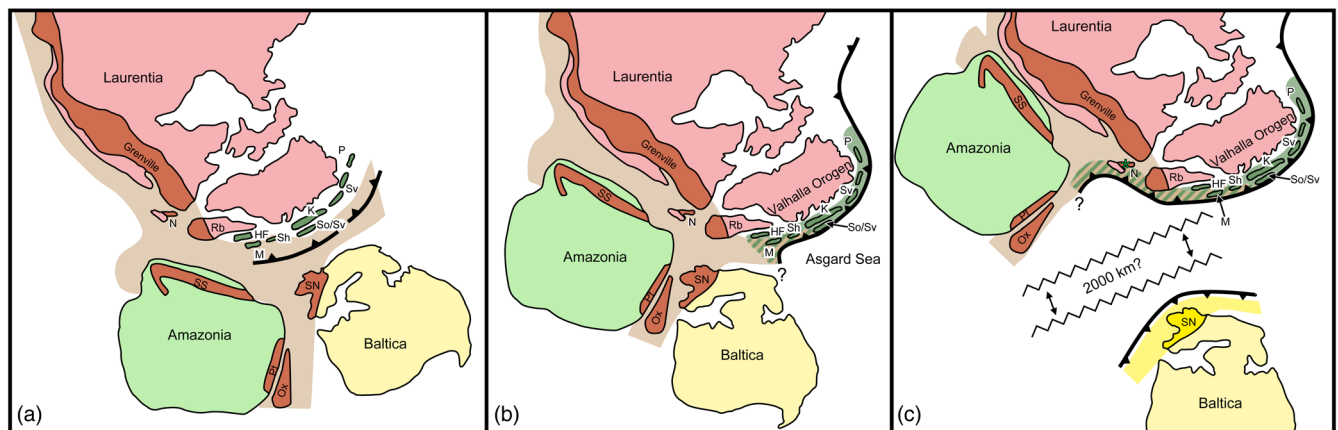

Fig. 17. (**a**–**c**) Alternative reconstructions of Laurentia, Baltica and Amazonia at *c.* 1000–950 Ma, following amalgamation of Rodinia and Grenville orogenesis, showing in green the approximate locations of Megasequence 1 successions (Olierook *et al.* 2020). HF, Hebridean foreland; K, Krummedal succession; M, 'Moine' metasedimentary rocks (including Wester Ross and Loch Ness supergroups); N, Newfoundland; Ox, Oaxaquia terrane; P, Pearya; Pt, Putumayo orogen; Rb, Rockall Bank; Sh, Shetland; SN, Sveconorwegian orogen; So/Sv, Sorøy and Sværholt successions; SS, Sunsas orogeny; Sv, Svalbard. Area of green diagonal shading in (**b**) and (**c**) represents overprinting of *c.* 970–930 Ma Valhalla tectonothermal activity in Scotland on Neoarchean basement that had been reworked at *c.* 1200–1000 Ma, as well as presumed overprinting of the Grenville orogen of Rockall Bank and Newfoundland. Green asterisk in (**c**) indicates location of *c.* 950 Ma volcanosedimentary rocks in northern Newfoundland (Strowbridge *et al.* 2022). Source: (b) modified from Cawood and Pisarevsky (2017).
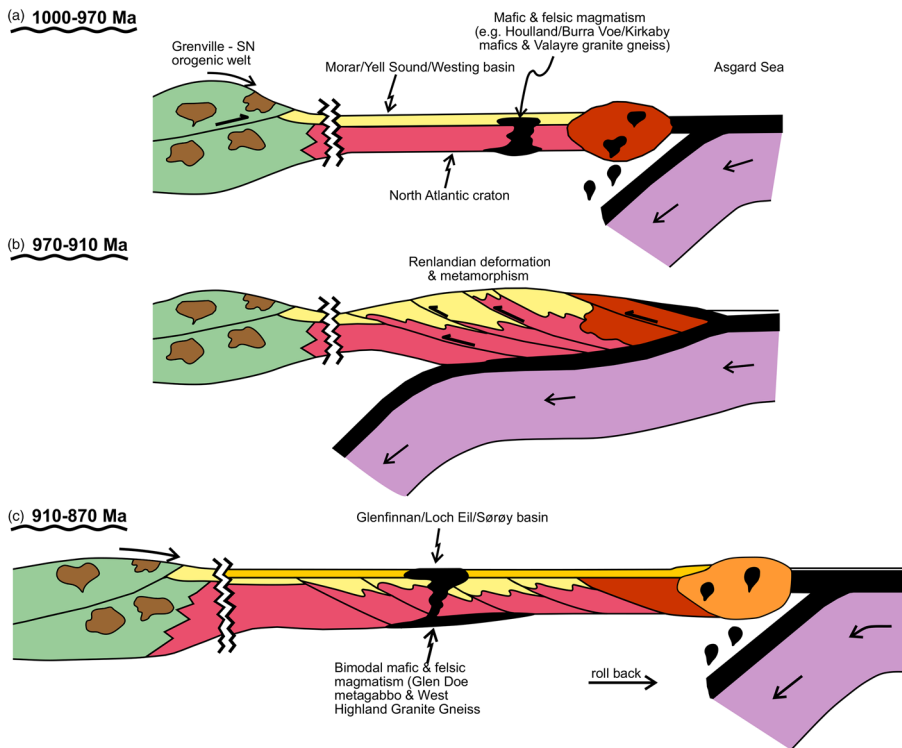
Fig. 18. Schematic plate-tectonic illustration for the NE Laurentian margin showing tectonic development in the period *c.* 1000–870 Ma.

An alternative scenario features a more southerly location of Baltica relative to Laurentia, with the accretionary Valhalla orogen (Cawood *et al.* 2010, 2015) developed along-strike between Pearya and Scotland (Fig. 17b; Cawood *et al.* 2010, 2015; Kirkland *et al.* 2011; Malone *et al.* 2014, 2017). However, it has also been argued on palaeomagnetic grounds that Baltica was entirely separate from Rodinia (Fig. 17c; Kulakov *et al.* 2022; Slagstad *et al.* 2023; Slagstad and Kulakov 2024). Recognition of *c.* 960–950 Ma arc-type magmatism intrusive into basement rocks of west Baltica suggests that a subduction zone dipped underneath this part of the craton and thus Laurentia and Baltica were separated by an oceanic tract at least during the early Tonian (Fig. 17c; Corfu 2019). If Baltica was not part of Rodinia during the Tonian, the Valhalla orogen may have extended as far as Newfoundland, where Strowbridge *et al.* (2022) documented a *c.* 950 Ma bimodal igneous suite (Fig. 17c). In this scenario, *c.* 1.2–1.0 Ga high-grade metamorphic events recorded in Archean basement inliers in mainland northern Scotland and Shetland (Storey *et al.* 2010; Strachan *et al.* 2020; Walker *et al.* 2021; Bird *et al.* 2023) require explanation. If Laurentia–Baltica collision is ruled out (Fig. 17c) then these events instead might correspond to a phase of accretionary orogenesis prior to or during the main Laurentia–Amazonia collision further west (Fig. 17c).

We favour reconstructions that feature a southerly location of western Baltica opposite Rockall Bank (Fig. 17b), although acknowledge that we have no evidence that can preclude a distal location of Baltica, at least during the Tonian (Fig. 17c). Our preferred tectonic model is that the Yell Sound and Westings groups and correlative successions of the Laurentian margin accumulated at *c.* 1000–970 Ma in marginal (back-arc *sensu lato*) basins located between the continental interior and an outboard subduction zone (Fig. 18a). The local presence in Scotland and Shetland of inliers of Archean basement indicates that these basins were probably floored by extended continental crust. Substantial influxes of sediment were derived from the erosion of the Grenvillian orogen and possibly also the Sveconorwegian orogen depending on the location of Baltica at this time. During the period *c.* 970–930 Ma, sediments were intruded by calc-alkaline magmas (Fig. 18a), and deformed and metamorphosed, although whether the latter resulted from flat-slab

subduction (Fig. 18b) or terrane accretion or a combination of the two is uncertain. We envisage that shallowing of the subducting slab resulted in continentward migration of the loci of calc-alkaline magmatism into the marginal basin, which was followed rapidly by crustal thickening (Fig. 18b), the Renlandian orogenic event of Cawood *et al.* (2010). Post-910 Ma subduction roll-back may then have thinned the previously thickened crust to produce successor basins that accommodated sedimentation of 'megasequence 2' successions (Fig. 18c). In Scotland, deposition of the Glenfinnan–Loch Eil–Badenoch groups was accompanied by *c.* 870 Ma bimodal magmatism (Fig. 18c; Millar 1999; Fowler *et al.* 2013). In Norway, the Sørøy succession was intruded by the products of a further episode of calc-alkaline magmatism at *c.* 840 Ma (Kirkland *et al.* 2006). Further phases of accretionary-style orogenesis within the period *c.* 840–725 Ma could account for the various pulses of orogenesis such as the Porsanger orogeny in Norway (Daly *et al.* 1991) and Knoydartian orogenic events in Scotland (Rogers *et al.* 1998; Vance *et al.* 1998; Cawood *et al.* 2010, 2015; Cutts *et al.* 2010). This broad tectonic scenario has many similarities to the orogenic record of various circum-Pacific marginal basins from the late Paleozoic onwards (e.g. Dalziel 1986; Collins 2002; Collins and Richards 2008; Klepeis *et al.* 2010). Comparisons might also be drawn with contemporary marginal basins of the west Pacific region, which are currently receiving sediment from the Mesozoic–Tertiary orogens of cratonic Asia. Future inboard migration of magmatism and accretionary-style orogenic activity would deform and metamorphose these sediments, potentially resulting in a tectonothermal record very similar to that displayed by the early Neoproterozoic successions of the NE Laurentian margin.

Conclusions

(1) The sedimentary protoliths of the Yell Sound Group (Shetland) and the metasedimentary rocks of the Naver Nappe (northern mainland Scotland) were deposited between *c.* 1005 and *c.* 960 Ma. Detrital zircons show a range of Paleoarchaean to Mesoproterozoic age clusters and unambiguous distinction between eastern Laurentian and Baltican sources is difficult.

(2) U–Pb zircon ages of *c.* 965–950 Ma obtained from meta-igneous rocks that intrude the Yell Sound and Westing groups and the Naver Nappe are interpreted as dating magmatic crystallization. Chemical discrimination diagrams and Hf and Nd isotope data together suggest that the protoliths of the mafic meta-igneous rocks were emplaced as relatively juvenile crustal contributions in an arc-related environment. The felsic melts probably resulted from advected heat provided by the mafic intrusions.

(3) Zircon growth at *c.* 920 Ma within the Yell Sound Group is linked with the *c.* 940–920 Ma high-grade 'Renlandian' metamorphic event documented previously within this unit (Jahn *et al.* 2017) and also the nearby Westing Group in Unst (Cutts *et al.* 2009b). Widespread evidence for later zircon growth and Pb loss at *c.* 470–460 Ma corresponds to the early Caledonian Grampian orogenic event recognized widely in Scotland and Ireland.

(4) The Yell Sound and Westing groups and the metasedimentary rocks of the Naver Nappe are broadly time-correlative with the Morar and Torridon groups of mainland northern Scotland and hence can be assigned to 'megasequence 1' of Olierook *et al.* (2020). Wider correlations include those with early Neoproterozoic metasedimentary successions of Ellesmere Island, East Greenland, NW, SW and East Svalbard, and the Laurentian-derived Kalak Nappe Complex of north Norway, all of which contain evidence for early Neoproterozoic felsic magmatism, some calc-alkaline in nature.

(5) The new data reported here indicate that early Neoproterozoic subduction-related magmatism and subsequent tectonism occurred at least as far south as the Scottish sector of the NE Laurentian margin. If Baltica formed part of Rodinia, this favours reconstructions that feature a southerly location of western Baltica opposite Rockall Bank. The Scottish margin of NE Laurentia would then be located relatively close to the periphery of Rodinia. The Yell Sound Group and correlative peri-Laurentian successions probably accumulated in a series of marginal basins floored by extended continental crust. They were subsequently intruded by arc-related magmas and deformed and metamorphosed during development of the Valhalla exterior accretionary orogen, part of a much more extensive peri-Rodinian subduction system.

Scientific editing by Yildirim Dilek

Author contributions **PDK**: conceptualization (equal), formal analysis (lead), investigation (equal), writing – original draft (equal), writing – review & editing (equal); **RAS**: conceptualization (equal), investigation (equal), writing – original draft (equal), writing – review & editing (equal); **MBF**: conceptualization (equal), formal analysis (equal), investigation (equal), writing – original draft (equal), writing – review & editing (equal); **EB**: conceptualization (supporting), formal analysis (supporting), writing – original draft (supporting), writing – review & editing (supporting); **ILM**: conceptualization (supporting), formal analysis (supporting), writing – original draft (supporting), writing – review & editing (supporting); **MH**: conceptualization (supporting), investigation (supporting), writing – original draft (supporting), writing – review & editing (supporting); **CC**: conceptualization (supporting), investigation (supporting), writing – original draft (supporting), writing – review & editing (supporting); **KAC**: conceptualization (supporting), investigation (supporting), writing – original draft (supporting), writing – review & editing (supporting).

Competing interests The authors declare that they have no known competing financial interests or personal relationships that could have appeared to influence the work reported in this paper.

Data availability All data generated or analysed during this study are included in this published article and its supplementary information files.

References

Abdelmalak, M.M., Andersen, T.B. *et al.* 2015. The ocean-continent in the mid-Norwegian margin: Insight from seismic data and an onshore Caledonian field analogue. *Geology*, **43**, 1011–1014, https://doi.org/10.1130/G37086.1

Baxter, E.F., Ague, J.J. and DePaolo, D.J. 2002. Prograde temperature–time evolution in the Barrovian type-locality constrained by Sm/Nd garnet ages from Glen Cova, Scotland. *Journal of the Geological Society, London*, **159**, 71–82, https://doi.org/10.1144/0016-76901013

Bingen, B., Andersson, J., Söderlund, U. and Möller, C. 2008. The Mesoproterozoic in the Nordic countries. *Episodes*, **31**, 29–34, https://doi.org/10.18814/epiiugs/2008/v31i1/005

Bingen, B., Belousova, E.A. and Griffin, W.L. 2011. Neoproterozoic recycling of the Sveconorwegian orogenic belt: detrital-zircon data from the Sparagmite basins in the Scandinavian Caledonides. *Precambrian Research*, **189**, 347–367, https://doi.org/10.1016/j.precamres.2011.07.005

Bingen, B., Viola, G., Möller, C., Auwera, J.V., Laurent, A. and Yi, K. 2020. The Sveconorwegian orogeny. *Gondwana Research*, **90**, 273–313, https://doi.org/10.1016/j.gr.2020.10.014

Bingen, B., Viola, G., Möller, C., Vander Auwera, J., Laurent, A. and Keewook, Y. 2021. The Sveconorwegian Orogeny. *Gondwana Research*, **90**, 273–313, https://doi.org/10.1016/j.gr.2020.10.014

Bird, A., Thirlwall, M., Strachan, R.A., Miller, I., Dempsey, E. and Hardman, K. 2023. Eclogites and basement terrane tectonics in the northern arm of the Grenville orogen, NW Scotland. *Geoscience Frontiers*, **14**, 101668, https://doi.org/10.1016/j.gsf.2023.101668

Bird, A.F., Cutts, K.A., Strachan, R.A., Thirlwall, M. and Hand, M. 2018. First evidence of Renlandian (*c.* 950 Ma) orogeny in Mainland Scotland: implications for circum-North Atlantic correlations and the status of the Moine Supergroup. *Precambrian Research*, **350**, 283–294, https://doi.org/10.1016/j.precamres.2017.12.019

Blichert-Toft, J. and Albarède, F. 1997. Separation of Hf and Lu for high-precision isotope analysis of rock samples by magnetic sector-multiple collector ICP-MS. *Contributions to Mineralogy and Petrology*, **127**, 248–260, https://doi.org/10.1007/s004100050278

Bonsor, H.C., Strachan, R.A., Prave, A.R. and Krabbendam, M. 2012. Sedimentology of the early Neoproterozoic Morar Group in northern Scotland: implications for basin models and tectonic setting. *Journal of the Geological Society, London*, **169**, 53–65, https://doi.org/10.1144/0016-76492011-039

British Geological Survey 1981. *Central Shetland. Scotland Sheet 128. Solid Edition*. 1:50,000 Geology Series. British Geological Survey, Keyworth, Nottingham.

British Geological Survey 1994. *Yell. Scotland Sheet 130. Solid and Drift Edition*. 1:50,000 Geology Series. British Geological Survey, Keyworth, Nottingham.

British Geological Survey 2004. *Northmaven. Scotland Sheet 129. Bedrock. 1:50,000 Geology Series*. British Geological Survey, Keyworth, Nottingham.

Burns, I.M. 1994. *Tectonothermal Evolution and Petrogenesis of the Naver and Kirtomy Nappes, North Sutherland*. PhD thesis, Oxford Brookes University.

Cawood, P.A. and Pisarevsky, S. 2006. Was Baltica right-way up or upside down in the Neoproterozoic? *Journal of the Geological Society, London*, **163**, 753–759, https://doi.org/10.1144/0016-76492005-126

Cawood, P.A. and Pisarevsky, S. 2017. Laurentia–Baltica–Amazonia relations during Rodinia assembly. *Precambrian Research*, **292**, 386–397, https://doi.org/10.1016/j.precamres.2017.01.031

Cawood, P.A., Nemchin, A.A., Strachan, R.A., Prave, A.R. and Krabbendam, M. 2007. Sedimentary basin and detrital zircon record along East Laurentia and Baltica during assembly and breakup of Rodinia. *Journal of the Geological Society, London*, **164**, 257–275, https://doi.org/10.1144/0016-76492006-115

Cawood, P.A., Strachan, R.A., Cutts, K.A., Kinny, P.D., Hand, M. and Pisarevsky, S. 2010. Neoproterozoic orogeny along the margin of Rodinia: Valhalla orogen, North Atlantic. *Geology*, **38**, 99–102, https://doi.org/10.1130/G30450.1

Cawood, P.A., Strachan, R.A. *et al.* 2015. Neoproterozoic to early Palaeozoic extensional and contractional history of East Laurentian margin sequences: the Moine Supergroup, Scottish Caledonides. *Geological Society of America Bulletin*, **127**, 349–371, https://doi.org/10.1130/B31068.1

Cawood, P.A., Strachan, R.A., Pisarevsky, S.A., Gladkochub, D.P. and Murphy, J.B. 2016. Linking collisional and accretionary orogenesis during Rodinia assembly and breakup: implications for models of supercontinent cycles. *Earth and Planetary Science Letters*, **440**, 118–126, https://doi.org/10.1016/j.epsl.2016.05.049

Chew, D. and Strachan, R.A. 2014. The Laurentian Caledonides of Scotland and Ireland. *Geological Society, London, Special Publications*, **390**, 45–91, https://doi.org/10.1144/SP390.16

Chew, D.M., Daly, J.S., Page, L.M. and Kennedy, M.J. 2003. Grampian orogenesis and the development of blueschist-facies metamorphism in western Ireland. *Journal of the Geological Society, London*, **160**, 911–924, https://doi.org/10.1144/0016-764903-012

Chew, D.M., Flowerdew, M.J., Page, L.M., Crowley, Q.G., Daly, J.S., Cooper, M. and Whitehouse, M.J. 2008. The tectonothermal evolution and provenance of the Tyrone Central Inlier, Ireland: Grampian imbrications of an outboard Laurentian microcontinent? *Journal of the Geological Society, London*, **165**, 675–685, https://doi.org/10.1144/0016-76492007-120

Chew, D.M., Daly, J.S., Magna, T., Page, L.M., Kirkland, C.L., Whitehouse, M.J. and Lam, R. 2010. Timing of ophiolite obduction in the Grampian orogen. *Geological Society of America Bulletin*, **122**, 1787–1799, https://doi.org/10.1130/B30139.1

Chu, N.-C., Taylor, R.N. *et al.* 2002. Hf isotope ratio analysis using multi-collector inductively coupled plasma mass spectrometry: an evaluation of isobaric interference corrections. *Journal of Analytical Atomic Spectroscopy*, **17**, 1567–1574, https://doi.org/10.1039/B206707B

Collins, W.S. 2002. Hot orogens, tectonic switching, and creation of continental crust. *Geology*, **30**, 535–538, https://doi.org/10.1130/0091-7613(2002)030<0535:HOTSAC>2.0.CO;2

Collins, W.S. and Richards, S.W. 2008. Geodynamic significance of S-type granites in circum-Pacific orogens. *Geology*, **36**, 559–562, https://doi.org/10.1130/G24658A.1

Corfu, F. 2019. The Sognefjell volcanic–subvolcanic complex – a late Sveconorwegian arc imbricated in the central Norwegian Caledonides. *Precambrian Research*, **331**, 105353, https://doi.org/10.1016/j.precamres.2019.105353

Cutts, K.A., Hand, M., Kelsey, D.E. and Strachan, R.A. 2009a. Orogenic versus extensional settings for regional metamorphism: Knoydartian events in the Moine Supergroup revisited. *Journal of the Geological Society, London*, **166**, 201–204, https://doi.org/10.1144/0016-76492008-015

Cutts, K.A., Hand, M., Kelsey, D.E., Wade, B., Strachan, R.A., Clark, C. and Netting, A. 2009b. Evidence for 930 Ma metamorphism in the Shetland Islands, Scottish Caledonides: implications for Neoproterozoic tectonics in the Laurentia–Baltica sector of Rodinia. *Journal of the Geological Society, London*, **166**, 1033–1048, https://doi.org/10.1144/0016-76492009-006

Cutts, K.A., Kinny, P.D. *et al.* 2010. Three metamorphic events recorded in a single garnet: coupled phase modelling with in situ LA-ICPMS, and SIMS geochronology from the Moine Supergroup, NW Scotland. *Journal of Metamorphic Geology*, **28**, 249–267, https://doi.org/10.1111/j.1525-1314.2009.00863.x

Cutts, K.A., Hand, M., Kelsey, D.E. and Strachan, R.A. 2011. *P–T* constraints and timing of Barrovian metamorphism in the Shetland Islands, Scottish Caledonides: implications for the structural setting of the Unst ophiolite. *Journal of the Geological Society, London*, **168**, 1265–1284, https://doi.org/10.1144/0016-76492010-165

Daly, J.S., Aitcheson, S.J., Cliff, R.A., Gayer, R.A. and Rice, A.H.N. 1991. Geochronological evidence from discordant plutons for a late Proterozoic orogen in the Caledonides of Finnmark, northern Norway. *Journal of the Geological Society, London*, **148**, 29–40, https://doi.org/10.1144/gsjgs.148.1.0029

Dalziel, I.W.D. 1986. Collision and Cordilleran orogenesis. *Geological Society, London, Special Publications*, **19**, 380–394, https://doi.org/10.1144/GSL.SP.1986.019.01.22

Dalziel, I.W.D. 1991. Pacific margins of Laurentia and East Antarctica–Australia as a conjugate rift pair: evidence and implications for an Eocambrian supercontinent. *Geology*, **19**, 598–601, https://doi.org/10.1130/0091-7613(1991)019<0598:PMOLAE>2.3.CO;2

DePaolo, D.J., Linn, A.M. and Schubert, G. 1991. The continental crustal age distribution – methods of determining mantle separation ages from Sm–Nd isotopic data and application to the south-western United States. *Journal of Geophysical Research*, **96**, 2071–2088, https://doi.org/10.1029/90JB02219

Dewey, J.F. and Ryan, P.D. 1990. The Ordovician evolution of the South Mayo Trough, western Ireland. *Tectonics*, **9**, 887–901, https://doi.org/10.1029/TC009i004p00887

Dewey, J.F. and Shackleton, R.M. 1984. A model for the evolution of the Grampian tract in the early Caledonides and Appalachians. *Nature*, **312**, 115–121, https://doi.org/10.1038/312115a0

Elming, S.A., Pisarevsky, S.A., Layer, P. and Bylund, G. 2014. A palaeomagnetic and $^{40}Ar/^{39}Ar$ study of mafic dykes in southern Sweden: a new Early Neoproterozoic key-pole for the Baltic Shield and implications for Sveconorwegian and Grenville loops. *Precambrian Research*, **244**, 192–206, https://doi.org/10.1016/j.precamres.2013.12.007

Flinn, D. 1985. The Caledonides of Shetland. *In*: Gee, D.G. and Sturt, B.A. (eds) *The Caledonide Orogen – Scandinavia and Related Areas*. Wiley, New York, 1159–1172.

Flinn, D. 1988. The Moine rocks of Shetland. *In*: Winchester, J.A. (ed.) *Later Proterozoic Stratigraphy of the Northern Atlantic Regions*. Blackie, Glasgow, 74–85.

Flinn, D. 1994. *Geology of Yell and Some Neighbouring Islands in Shetland. Memoir of the British Geological Survey, Sheet 130 (Scotland)*. HMSO, London.

Flinn, D. 2007. The Dalradian rocks of Shetland their implications for the plate tectonics of the northern Iapetus. *Scottish Journal of Geology*, **43**, 124–142, https://doi.org/10.1144/sjg43020125

Flinn, D. 2014. *Geology of Unst and Fetlar in Shetland. Memoir of the British Geological Survey, Sheet 131 (Scotland)*. HMSO, London.

Flinn, D., Frank, P.L., Brook, M. and Pringle, I.R. 1979. Basement–cover relations in Shetland. *Geological Society, London, Special Publications*, **8**, 109–115, https://doi.org/10.1144/GSL.SP.1979.008.01.09

Fowler, M.B., Millar, I.L., Strachan, R.A. and Fallick, A.E. 2013. Petrogenesis of the Neoproterozoic West Highland Granitic Gneiss, Scottish Caledonides: cryptic mantle input to S-type granites? *Lithos*, **168**, 173–185, https://doi.org/10.1016/j.lithos.2013.02.010

Friedrich, A.M., Hodges, K.V., Bowring, S.A. and Martin, M.W. 1999. Geochronological constraints on the magmatic, metamorphic and thermal evolution of the Connemara Caledonides, western Ireland. *Journal of the Geological Society, London*, **156**, 1217–1230, https://doi.org/10.1144/gsjgs.156.6.1217

Friend, C.R.L., Jones, K.A. and Burns, I.M. 2000. New high-pressure granulite facies event in the Moine Supergroup, northern Scotland: implications for Taconic (early Caledonian) crustal evolution. *Geology*, **28**, 543–546, https://doi.org/10.1130/0091-7613(2000)28<543:NHGEIT>2.0.CO;2

Friend, C.R.L., Strachan, R.A. and Kinny, P.D. 2008. U–Pb zircon dating of basement inliers within the Moine Supergroup, Scottish Caledonides: implications of Archaean protolith ages. *Journal of the Geological Society, London*, **165**, 807–815, https://doi.org/10.1144/0016-76492007-125

Gasser, D. and Andresen, A. 2013. Caledonian terrane amalgamation of Svalbard: detrital zircon provenance of Mesoproterozoic to Carboniferous strata from Oscar II Land, western Spitsbergen. *Geological Magazine*, **150**, 1103–1126, https://doi.org/10.1017/S0016756813000174

Gasser and Andresen 2014 (details to be added by author).

Ge, R., Zhu, W. and Wilde, S. 2016. Mid-Neoproterozoic (ca. 830–800 Ma) metamorphic P–T paths link Tarim to the circum-Rodinia subduction–accretion system. *Tectonics*, **35**, 1465–1488, https://doi.org/10.1002/2016TC004177

Gee, D.G., Johansson, A. *et al.* 1995. Grenvillian basement and a major unconformity within the Caledonides of Nordaustlandet, Svalbard. *Precambrian Research*, **70**, 215–234, https://doi.org/10.1016/0301-9268(94)00041-O

Gee, D.G., Andréasson, P.-G., Lorenz, H., Frei, D. and Majka, J. 2015. Detrital zircon signatures of the Baltoscandian margin along the Arctic Circle Caledonides in Sweden: the Sveconorwegian connection. *Precambrian Research*, **265**, 40–56, https://doi.org/10.1016/j.precamres.2015.05.012

Gower, C.F., Kamo, S. and Krogh, T. 2008. Indentor tectonism in the eastern Grenville Province. *Precambrian Research*, **167**, 201–212, https://doi.org/10.1016/j.precamres.2008.08.004

Griffin, W.L., Pearson, N.J., Belousova, E., Jackson, S.E., O'Reilly, S.Y., van Achterberg, E. and Shee, S.R. 2000. The Hf isotope composition of cratonic mantle: LAM-MC-ICPMS analysis of zircon megacrysts in kimberlites. *Geochemica et Cosmochimica Acta*, **64**, 133–147, https://doi.org/10.1016/S0016-7037(99)00343-9

Griffin, W.L., Belousova, E.A., Shee, S.R., Rearson, N.J. and O'Reilly, S.Y. 2004. Archean crustal evolution in the northern Yilgarn Craton: U–Pb and Hf-isotope evidence from detrital zircons. *Precambrian Research*, **127**, 19–41, https://doi.org/10.1016/j.precamres.2003.12.011

Hoffman, P.F. 1991. Did the breakout of Laurentia turn Gondwanaland inside-out? *Science*, **252**, 1409–1412, https://doi.org/10.1126/science.252.5011.1409

Holdsworth, R.E., Strachan, R.A. and Harris, A.L. 1994. Precambrian rocks in northern Scotland east of the Moine Thrust: the Moine Supergroup. *Geological Society, London, Special Report*, **22**, 23–32.

Holdsworth, R.E., Strachan, R.A. and Alsop, G.I. 2001. *Geology of the Tongue District. Memoir of the British Geological Survey*. HMSO.

Holdsworth, R.E., Morton, A. *et al.* 2019. The nature and significance of the Faroe–Shetland Terrane: linking Archaean basement blocks across the North Atlantic. *Precambrian Research*, **321**, 154–171, https://doi.org/10.1016/j.precamres.2018.12.004

Jackson, S.E., Pearson, N.J., Griffin, W.L. and Belousova, E.A. 2004. The application of laser ablation-inductively coupled plasma-mass spectrometry to in situ U–Pb zircon geochronology. *Chemical Geology*, **211**, 47–69, https://doi.org/10.1016/j.chemgeo.2004.06.017

Jahn, I., Strachan, R.A., Fowler, M.B., Bruand, E., Kinny, P.D., Clark, C. and Taylor, R.J.M. 2017. Evidence from U–Pb zircon geochronology for early Neoproterozoic (Tonian) reworking of an Archaean inlier in northeastern Shetland, Scottish Caledonides. *Journal of the Geological Society, London*, **174**, 217–232, https://doi.org/10.1144/jgs2016-054

Johansson, A. 2009. Baltica, Amazonia and the SAMBA connection – 1000 million years of neighbourhood during the Proterozoic? *Precambrian Research*, **175**, 221–234, https://doi.org/10.1016/j.precamres.2009.09.011

Johansson, A. 2014. From Rodinia to Gondwana with the 'SBA' model – a distant view from Baltica towards Amazonia and beyond. *Precambrian Research*, **244**, 226–235, https://doi.org/10.1016/j.precamres.2013.10.012

Johansson, A. 2016. Comments to "Detrital zircon signatures of the Baltoscandian margin along the Arctic Circle Caledonides in Sweden: the Sveconorwegian connection". *Precambrian Research*, **276**, 233–235, https://doi.org/10.1016/j.precamres.2015.12.006

Johansson, A., Larionov, A.N., Teben'kov, A.M., Gee, D.G., Whitehouse, M.J. and Vestin, J. 1999. Grenvillian magmatism of western and central

Nordaustlandet, northeastern Svalbard. *Transactions of the Royal Society of Edinburgh: Earth Sciences*, **90**, 221–254, https://doi.org/10.1017/S0263593300002583

Johansson, A., Larionov, A.N., Gee, D.G., Ohta, Y., Teben'kov, A.M. and Sandelin, S. 2004. Grenvillian and Caledonian tectono-magmatic activity in northeasternmost Svalbard. *Geological Society of London, Memoirs*, **30**, 207–232, https://doi.org/10.1144/GSL.MEM.2004.030.01.17

Johansson, A., Gee, D.G., Larionov, A.N., Ohta, Y. and Tebenkov, A.M. 2005. Grenvillian and Caledonian evolution of eastern Svalbard – a tale of two orogenies. *Terra Nova*, **17**, 317–325, https://doi.org/10.1111/j.1365-3121.2005.00616.x

Kalsbeek, F., Thrane, K., Nutman, A.P. and Jepsen, H.F. 2000. Late Mesoproterozoic to early Neoproterozoic history of the East Greenland Caledonides: evidence for Grenvillian orogenesis. *Journal of the Geological Society, London*, **157**, 1215–1225, https://doi.org/10.1144/jgs.157.6.1215

Kinny, P.D., Friend, C.R.L., Strachan, R.A., Watt, G.R. and Burns, I.M. 1999. U–Pb geochronology of regional migmatites, East Sutherland, Scotland: evidence for crustal melting during the Caledonian orogeny. *Journal of the Geological Society, London*, **156**, 1143–1152, https://doi.org/10.1144/gsjgs.156.6.1143

Kinny, P.D., Strachan, R.A. *et al.* 2019. The Neoarchean Uyea Gneiss Complex, Shetland: an onshore fragment of the Rae Craton on the European Plate. *Journal of the Geological Society, London*, **176**, 847–862, https://doi.org/10.1144/jgs2019-017

Kirkland, C.L., Daly, J.S. and Whitehouse, M.J. 2006. Granitic magmatism of Grenvillian and late Neoproterozoic age in Finnmark, Arctic Norway: constraining pre-Scandian deformation in the Kalak Nappe Complex. *Precambrian Research*, **145**, 24–52, https://doi.org/10.1016/j.precamres.2005.11.012

Kirkland, C.L., Daly, J.S. and Whitehouse, M.J. 2007. Provenance and terrane evolution of the Kalak Nappe complex, Norwegian Caledonides: implications for Neoproterozoic palaeogeography and tectonics. *Journal of Geology*, **115**, 21–41, https://doi.org/10.1086/509247

Kirkland, C.L., Daly, J.S. and Whitehouse, M.J. 2008*a*. Basement–cover relationships of the Kalak Nappe Complex, Arctic Norwegian Caledonides and constraints on Neoproterozoic terrane assembly in the North Atlantic region. *Precambrian Research*, **160**, 245–276, https://doi.org/10.1016/j.precamres.2007.07.006

Kirkland, C.L., Strachan, R.A. and Prave, A.R. 2008*b*. Detrital zircon signature of the Moine Supergroup, Scotland: contrasts and comparisons with other Neoproterozoic successions within the circum-North Atlantic region. *Precambrian Research*, **163**, 332–350, https://doi.org/10.1016/j.precamres.2008.01.003

Kirkland, C.L., Bingen, B., Whitehouse, M.J., Beyer, E. and Griffin, W.L. 2011. Neoproterozoic palaeogeography in the North Atlantic region: inference from the Akkajaure and Seve Nappes of the Scandinavian Caledonides. *Precambrian Research*, **186**, 127–146, https://doi.org/10.1016/j.precamres.2011.01.010

Klepeis, K., Betka, P. *et al.* 2010. Continental underthrusting and obduction during the Cretaceous closure of the Rocas Verdes rift basin, Cordillera Darwin, Patagonian Andes. *Tectonics*, **29**, TC3014, https://doi.org/10.1029/2009TC002610

Krabbendam, M., Prave, A.R. and Cheer, D. 2008. A fluvial origin for the Neoproterozoic Morar Group, NW Scotland: implications for Torridon–Morar group correlation and the Grenville Orogen Foreland Basin. *Journal of the Geological Society, London*, **165**, 379–394, https://doi.org/10.1144/0016-76492007-076

Krabbendam, M., Bonsor, H., Horstwood, M.S.A. and Rivers, T. 2017. Tracking the evolution of the Grenvillian foreland basin: constraints from sedimentology and detrital zircon and rutile in the Sleat and Torridon groups, Scotland. *Precambrian Research*, **295**, 67–89, https://doi.org/10.1016/j.precamres.2017.04.027

Krabbendam, M., Strachan, R.A. and Prave, A.R. 2021. A new stratigraphic framework for the early Neoproterozoic successions of Scotland. *Journal of the Geological Society, London*, **178**, jgs2021-054, https://doi.org/10.1144/jgs2021-054

Kulakov, E.V., Slagstad, T., Ganerød, M. and Torsvik, T.H. 2022. Paleomagnetism and ^{40}Ar/^{39}Ar geochronology of Meso-Neoproterozoic rocks from southwest Norway. Implications for magnetic remanence ages and the paleogeography of Baltica in a Rodinia supercontinent context. *Precambrian Research*, **379**, 106786, https://doi.org/10.1016/j.precamres.2022.106786

Lambert, R.St.J. and McKerrow, W.S. 1976. The Grampian Orogeny. *Scottish Journal of Geology*, **12**, 271–292, https://doi.org/10.1144/sjg12040271

Laurent, O., Martin, H., Moyen, J.F. and Doucelance, R. 2014. The diversity and evolution of late-Archean granitoids: evidence for the onset of "modern-style" plate tectonics between 3.0 and 2.5 Ga. *Lithos*, **205**, 208–235, https://doi.org/10.1016/j.lithos.2014.06.012

Law, R.D., Strachan, R.A., Thirlwall, M. and Thigpen, J.R. 2024. The Caledonian Orogeny: late Ordovician to early Devonian tectonic and magmatic events associated with closure of the Iapetus Ocean. *In*: Smith, M. and Strachan, R.A. (eds) *The Geology of Scotland*, 5th edn. Geological Society, London, 205–257.

Leslie, A.G. and Nutman, A.P. 2003. Evidence for Neoproterozoic orogenesis and early high temperature Scandian deformation events in the southern East Greenland Caledonides. *Geological Magazine*, **140**, 309–333, https://doi.org/10.1017/S0016756803007593

Leslie, A.G., Stone, P. and Strachan, R.A. 2024. Early to Middle Ordovician Grampian orogenesis: ophiolite obduction and arc–continent collision. *In*: Smith, M. and Strachan, R.A. (eds) *The Geology of Scotland*, 5th edn. Geological Society, London, 139–170.

Li, Z.X., Bogdanova, S.V. *et al.* 2008. Assembly, configuration, and break-up history of Rodinia: a synthesis. *Precambrian Research*, **160**, 179–210, https://doi.org/10.1016/j.precamres.2007.04.021

Lorenz, H., Gee, D.G., Larionov, A.N. and Majka, J. 2012. The Grenville–Sveconorwegian orogen in the high Arctic. *Geological Magazine*, **149**, 875–891, https://doi.org/10.1017/S0016756811001130

Ludwig, K.R. 2003. *Isoplot 3.00. A geochronological toolkit for Microsoft Excel*. Berkeley Geochronological Center, Special Publication, 4a.

Ludwig, K.R. 2009. *Squid 2.50, A User's Manual*. Berkeley Geochronology Centre, Berkeley, CA, unpublished report.

Majka, J., Be'Eri-Shlevin, Y., Gee, D.G., Czerny, J., Frei, D. and Ladenberger, A. 2014. Torellian (*c.* 640 Ma) metamorphic overprint of Tonian (*c.* 950 Ma) basement in the Caledonides of southwestern Svalbard. *Geological Magazine*, **151**, 732–748, https://doi.org/10.1017/S0016756813000794

Malone, S.J., McClelland, W.C., von Gosen, W. and Piepjohn, K. 2014. Proterozoic Evolution of the North Atlantic–Arctic Caledonides: insights from Detrital Zircon Analysis of Metasedimentary Rocks from the Pearya Terrane, Canadian High Arctic. *Journal of Geology*, **122**, 623–647, https://doi.org/10.1086/677902

Malone, S.J., McClelland, W.C., von Gosen, W. and Piepjohn, K. 2017. The earliest Neoproterozoic magmatic record of the Pearya Terrane, Canadian High Arctic: implications for terrane reconstructions in the Arctic Caledonides. *Precambrian Research*, **292**, 323–349, https://doi.org/10.1016/j.precamres.2017.01.006

McClelland, W.C., von Gosen, W. and Piepjohn, K. 2018. Tonian and Silurian magmatism in Nordaustlandet: Svalbard's place in the Caledonian orogen. *Geological Society of America, Special Papers*, **541**, 63–80, https://doi.org/10.1130/2018.2541(04)

Meschede, M. 1986. A method of discriminating between different types of mid-ocean ridge basalts and continental tholeiites with the Nb–Zr–Y diagram. *Chemical Geology*, **56**, 207–218, https://doi.org/10.1016/0009-2541(86)90004-5

Millar, I.L. 1999. Neoproterozoic extensional magmatism associated with the West Highland granite gneiss in the Moine Supergroup of NW Scotland. *Journal of the Geological Society, London*, **156**, 1153–1162, https://doi.org/10.1144/gsjgs.156.6.1153

Moorhouse, S.J. and Moorhouse, V.E. 1988. The Moine Assemblage in Sutherland. *In*: Winchester, J.A. (ed.) *Later Proterozoic Stratigraphy in the Northern Atlantic Regions*. Blackie, Glasgow, 54–73.

Nasdala, L., Hofmeister, W. *et al.* 2008. Zircon M257 – a homogeneous natural reference material for the ion microprobe U–Pb analysis of zircon. *Geostandards and Geoanalytical Research*, **32**, 247–265, https://doi.org/10.1111/j.1751-908X.2008.00914.x

Nystuen, J.P., Andresen, A., Kumpulainen, R.A. and Siedlecka, A. 2008. Neoproterozoic basin evolution in Fennoscandinavia, East Greenland and Svalbard. *Episodes*, **31**, 1.

Olierook, H.K.H., Barham, M., Kirkland, C.L., Hollis, J. and Vass, A. 2020. Zircon fingerprint of the Neoproterozoic North Atlantic: perspectives from East Greenland. *Precambrian Research*, **342**, 105653, https://doi.org/10.1016/j.precamres.2020.105653

Oliver, G.J.H., Chen, F., Buchwaldt, R. and Hegner, E. 2000. Fast tectonometamorphism and exhumation in the type area of the Barrovian and Buchan zones. *Geology*, **28**, 459–462, https://doi.org/10.1130/0091-7613(2000)28<459:FTAEIT>2.0.CO;2

Paquette, J.-L., Piro, J.-L., Devidal, J.-L., Bosse, V. and Didier, A. 2014. Sensitivity enhancement in LA-ICP-MS by N$_2$ addition to carrier gas: application to radiometric dating of U–Th-bearing minerals. *Agilent ICPMS Journal*, **58**, 4–5.

Park, R.G. 1992. Plate kinematic history of Baltica during the Middle to Late Proterozoic: a model. *Geology*, **20**, 725–728, https://doi.org/10.1130/0091-7613(1992)020<0725:PKOHOBD>2.3.CO;2

Pearce, J.A. 2008. Geochemical fingerprinting of oceanic basalts with applications to ophiolite classification and the search for Archean oceanic crust. *Lithos*, **100**, 14–48, https://doi.org/10.1016/j.lithos.2007.06.016

Pease, V., Gee, D.G., Vernikovsky, V., Vernikovskaya, A. and Kireev, S. 2001. The Mamont–Shrenk terrane: a Mesoproterozoic complex in the Neoproterozoic accretionary belt of central Taimyr, Northern Siberia. *Terra Nova*, **13**, 270–280, https://doi.org/10.1046/j.1365-3121.2001.00351.x

Pettersson, C.H., Tenenkov, A.M., Larionov, A.N., Andresen, A. and Pease, V. 2009. Timing of migmatization and granite genesis in the Northwestern Terrane of Svalbard, Norway: implications for regional correlations in the Arctic Caledonides. *Journal of the Geological Society, London*, **166**, 147–158, https://doi.org/10.1144/0016-76492008-023

Peucat, J.J., Ohta, Y., Gee, D.G. and Bernard-Griffiths, J. 1989. U/Pb, Sr and Nd evidence for Grenvillian and latest Proterozoic tectonothermal activity in the Spitzbergen Caledonides, Arctic Ocean. *Lithos*, **22**, 275–285, https://doi.org/10.1016/0024-4937(89)90030-3

Prave, A.R., Fallick, A.E., Strachan, R.A., Krabbendam, M. and Leslie, A.G. 2024. Middle Neoproterozoic to early Ordovician: foreland basins, climatic

extremes and rift-to-drift margins. *In*: Smith, M. and Strachan, R.A. (eds) *The Geology of Scotland*, 5th edn. Geological Society, London, 111–138.

Rogers, G., Hyslop, E.K., Strachan, R.A., Paterson, B.A. and Holdsworth, R.E. 1998. The structural setting and U–Pb geochronology of Knoydartian pegmatites in W. Inverness-shire: evidence for Neoproterozoic tectonothermal events in the Moine of NW Scotland. *Journal of the Geological Society, London*, **155**, 685–696, https://doi.org/10.1144/gsjgs.155.4.0685

Scherer, E., Munker, C. and Mezger, K. 2001. Calibration of the lutetium–hafnium clock. *Science*, **293**, 683–687, https://doi.org/10.1126/science.1061372

Slagstad, T. and Kirkland, C.L. 2017. The use of detrital zircon data in terrane analysis: a nonunique answer to provenance and tectonostratigraphic position in the Scandinavian Caledonides. *Lithosphere*, **9**, 1002–1011, https://doi.org/10.1130/l663.1

Slagstad, T. and Kulakov, E.V. 2024. Rodinia without Baltica? Constraints from Sveconorwegian orogenic style and palaeomagnetic data. *Geological Society, London, Special Publications*, **542**, 87–104, https://doi.org/10.1144/SP542-2022-330

Slagstad, T., Kulakov, E.V., Anderson, M.W., Saalmann, K., Kirkland, C.L., Henderson, I.H.C. and Ganerød, M. 2023. Was Baltica part of Rodinia? *Terra Nova*, **35**, 167–173, https://doi.org/10.1111/ter.12640

Stern, R. 2001. *A New Isotopic and Trace-Element Standard for the Ion-Microprobe: Preliminary Thermal Ionisation Mass Spectrometry (TIMS) U–Pb and Electron Microprobe Data*. Geological Survey of Canada, Radiogenic Age and Isotope Studies, Report **14**. Current Research, **2001-F1**.

Stern, R.A., Bodorkos, S., Kamo, S.L., Hickman, A.H. and Corfu, F. 2009. Measurement of SIMS instrumental mass fractionation of Pb isotopes during zircon dating. *Geostandards and Geoanalytical Research*, **33**, 145–168, https://doi.org/10.1111/j.1751-908X.2009.00023.x

Štípská, P., Peřestý, V. *et al.* 2023. Anticlockwise metamorphic paths at ca. 890–790 Ma from the NE Baidrag block, Mongolia, indicate back-arc compression at the Rodinia periphery. *Geoscience Frontiers*, **14**, 101520, https://doi.org/10.1016/j.gsf.2022.101520

Storey, C.D., Brewer, T.S., Anczkiewicz, R., Parrish, R.R. and Thirlwall, M.F. 2010. Multiple high-pressure metamorphic events and crustal telescoping in the NW Highlands of Scotland. *Journal of the Geological Society, London*, **167**, 455–468, https://doi.org/10.1144/0016-76492009-024

Strachan, R.A. and Holdsworth, R.E. 1988. Basement–cover relationships and structure within the Moine rocks of central and southeast Sutherland. *Journal of the Geological Society, London*, **145**, 23–36, https://doi.org/10.1144/gsjgs.145.1.0023

Strachan, R.A., Nutman, A.P. and Friderichsen, J.D. 1995. SHRIMP U–Pb geochronology and metamorphic history of the Smallefjord Sequence, NE Greenland Caledonides. *Journal of the Geological Society, London*, **152**, 779–784, https://doi.org/10.1144/gsjgs.152.5.0779

Strachan, R.A., Smith, M., Harris, A.L. and Fettes, D.J. 2002. The Northern Highland and Grampian terranes. *In*: Trewin, N. (ed.) *Geology of Scotland*, 4th edn. Geological Society, London, 81–147.

Strachan, R.A., Holdsworth, R.E., Friend, C.R.L., Burns, I.M. and Alsop, G.I. 2010*a*. Excursion 13: North Sutherland. *In*: Strachan, R.A., Friend, C.R.L., Alsop, G.I. and Miller, S. (eds) *An Excursion Guide to the Moine Geology of the Northern Highlands of Scotland*. Scottish Academic Press, 231–265.

Strachan, R.A., Holdsworth, R.E., Krabbendam, M. and Alsop, G.I. 2010*b*. The Moine Supergroup of NW Scotland: insights into the analysis of polyorogenic supracrustal sequences. *Geological Society, London, Special Publications*, **335**, 233–254, https://doi.org/10.1144/SP335.11

Strachan, R.A., Prave, A.R., Kirkland, C.R. and Storey, C.D. 2013. U–Pb detrital zircon geochronology and regional correlation of the Dalradian Supergroup, Shetland Islands, Scotland: implications for late Neoproterozoic–Cambrian basin development along the eastern margin of Laurentia. *Journal of the Geological Society, London*, **170**, 905–916, https://doi.org/10.1144/jgs2013-057

Strachan, R.A., Johnson, T.E., Kirkland, C.L., Kinny, P.D. and Kusky, T. 2020. A Baltic heritage in Scotland: basement terrane transfer during the Grenville Orogeny. *Geology*, **48**, 1094–1098, https://doi.org/10.1130/G47615.1

Strachan, R.A., Kirkland, C.L., Finlay, A.J., Wray, D.S., Metcalfe, J.H. and Holdsworth, R.E. 2024a. U–Pb apatite geochronology shows multiple thermal overprints within the Neoarchean foreland basement of the Faroe–Shetland Terrane. *Journal of the Geological Society, London*, **181**, https://doi.org/10.1144/jgs2024-003

Strachan, R.A., Prave, A.R., Krabbendam, M. and Smith, M. 2024b. Late Mesoproterozoic to Middle Neoproterozoic sedimentation and orogeny. *In*: Smith, M. and Strachan, R.A. (eds) *The Geology of Scotland*, 5th edn. Geological Society, London, 81–110.

Strowbridge, S., Indares, A., Dunning, G. and Wälle, M. 2022. A Tonian volcano-sedimentary succession in Newfoundland, eastern North America: a post-Grenvillian link to the Asgard Sea? *Geology*, **50**, 655–659, https://doi.org/10.1130/G49885.1

Sun, S.S. and McDonough, W.F. 1989. Chemical and isotopic systematics of oceanic basalts: implications for mantle compositions and processes. *Geological Society, London, Special Publications*, **42**, 313–345, https://doi.org/10.1144/GSL.SP.1989.042.01.17

Torsvik, T.H. 2003. The Rodinia Jigsaw Puzzle. *Science*, **300**, 1379–1381, https://doi.org/10.1126/science.1083469

Trettin, H.P., Parrish, R.R. and Roddick, J.C. 1992. New U–Pb and $^{40}Ar/^{39}Ar$ age determinations from northern Ellesmere and Axel Heiberg islands, Northwest Territories and their tectonic significance. *Geological Survey of Canada Papers*, **92-2**, 3–30.

Van Achterbergh, E., Griffin, C.G. and Ryan, W.L. 2001. Conference Paper: GLITTER: on-line interactive data reduction for the Laser Ablation ICP-MS Microprobe Conference Paper. *In*: Ninth Annual V. M. Goldschmidt Conference, Cambridge.

Vance, D., Strachan, R.A. and Jones, K.A. 1998. Extensional versus compressional settings for metamorphism, garnet chronometry and pressure–temperature–time histories in the Moine Supergroup, northwest Scotland. *Geology*, **26**, 927–930, https://doi.org/10.1130/00917613(1998)026<0927;EVCSFM>2.3.CO;2

Van Staal, C.R., Dewey, J.F., MacNiocaill, C. and McKerrow, W.S. 1998. The Cambrian–Silurian tectonic evolution of the northern Appalachians: history of a complex, southwest Pacific-type segment of Iapetus. *Geological Society, London, Special Publications*, **143**, 199–242, https://doi.org/10.1144/GSL.SP.1998.143.01.17

Van Staal, C.R., Whalen, J.B., Valverde-Vaquero, P., Zagorevski, A. and Rogers, N. 2009. Pre-Carboniferous, episodic accretion-related, orogenesis along the Laurentian margin of the northern Appalachians. *Geological Society, London, Special Publications*, **327**, 271–316, https://doi.org/10.1144/SP327.13

Vermeesch, P. 2018. IsoplotR: a free and open toolbox for geochronology. *Geoscience Frontiers*, **9**, 1479–1493, https://doi.org/10.1016/j.gsf.2018.04.001

Vernikovsky, V.A., Metelkin, D.V., Vernikovskaya, A.E., Sal'nikova, E.B., Kovach, V.P. and Kotov, A.B. 2011. The oldest island arc complex of Taimyr: concerning the issue of the Central-Taimyr accretionary belt formation and palaeogeodynamic reconstructions in the Arctic. *Doklady Earth Sciences*, **436**, 186–192, https://doi.org/10.1134/S1028334X1102019X

Walker, S., Thirlwall, M.F., Strachan, R.A. and Bird, A.F. 2016. Evidence from Rb–Sr mineral ages for multiple orogenic events in Caledonides of the Shetland Islands, Scotland. *Journal of the Geological Society, London*, **173**, 489–503, https://doi.org/10.1144/jgs2015-034

Walker, S., Bird, A.F., Thirlwall, M.F. and Strachan, R.A. 2021. Caledonian and pre-Caledonian orogenic events in Shetland, Scotland: evidence from garnet Lu–Hf and Sm–Nd geochronology. *Geological Society, London, Special Publications*, **503**, 305–331, https://doi.org/10.1144/SP503-2020-022

Watt, G.R. and Thrane, K. 2001. Early Neoproterozoic events in East Greenland. *Precambrian Research*, **110**, 165–184, https://doi.org/10.1016/S0301-9268(01)00186-3

Watt, G.R., Kinny, P.D. and Friderichsen, J.D. 2000. U–Pb geochronology of Neoproterozoic and Caledonian tectonothermal events in the East Greenland Caledonides. *Journal of the Geological Society, London*, **157**, 1031–1048, https://doi.org/10.1144/jgs.157.5.1031

Weil, A.B., Van der Voo, R., MacNiocall, C. and Meert, G.M. 1998. The Proterozoic supercontinent Rodinia: palaeomagnetically derived reconstructions for the 1100 to 800 Ma interval. *Earth and Planetary Science Letters*, **154**, 13–24, https://doi.org/10.1016/S0012-821X(97)00127-1

Wiedenbeck, M., Allé, P. and Corfu, F. 1995. Three Natural Zircon Standards for U–Th–Pb, Lu–Hf, trace element and REEAnalyses. *Geostandards Newsletter*, **19**, 1–23, https://doi.org/10.1111/j.1751-908X.1995.tb00147.x

Wood, D.A. 1980. The application of a Th–Hf–Ta diagram to problems of tectonomagmatic classification and to establishing the nature of crustal contamination of basaltic lavas of the British Tertiary volcanic complex. *Earth and Planetary Science Letters*, **50**, 11–30, https://doi.org/10.1016/0012-821X(80)90116-8

Woodhead, J.D. and Hergt, J.M. 2005. A preliminary appraisal of seven natural zircon reference materials for in situ Hf isotope determination. *Geostandards and Geoanalytical Research*, **29**, 183–195, https://doi.org/10.1111/j.1751-908X.2005.tb00891.x

Woodhead, J.D., Hergt, J.M., Shelley, M., Eggins, S. and Kemp, R. 2004. Zircon Hf isotope analysis with an excimer laser, depth profiling, ablation of complex geometries and concomitant age estimation. *Chemical Geology*, **209**, 121–135, https://doi.org/10.1016/j.chemgeo.2004.04.026